Mathematical Biosciences and Engineering

https://www.aimspress.com/journal/mbe

MBE, 21(11): 7554–7581.
DOI: 10.3934/mbe.2024332
Received: 05 August 2024
Revised: 10 October 2024
Accepted: 04 November 2024
Published: 13 November 2024

Research article

A mathematical model of flavescence dorée in grapevines by considering seasonality

Fernando Huancas[1,*], Aníbal Coronel[2,*], Rodolfo Vidal[1], Stefan Berres[3,4] and Humberto Brito[1]

[1] Departamento de Matemática, Facultad de Ciencias Naturales, Matemáticas y del Medio Ambiente, Universidad Tecnológica Metropolitana, Las Palmeras No. 3360, Ñuñoa-Santiago 7750000, Chile

[2] GMA, Departamento de Ciencias Básicas-Centro de Ciencias Exactas CCE-UBB, Facultad de Ciencias, Universidad del Bío-Bío, Campus Fernando May, Chillán 3780000, Chile

[3] Núcleo de Investigación en Bioproductos y Materiales Avanzados (BioMA), Universidad Católica de Temuco, Temuco 4780002, Chile

[4] Integrata-Stiftung für humane Nutzung der Informationstechnologie, Vor dem Kreuzberg 28, 72070 Tübingen, Deutschland

* **Correspondence:** Email: fhuancas@utem.cl, acoronel@ubiobio.cl.

Abstract: This paper presents a mathematical model to describe the spread of flavescence dorée, a disease caused by the bacterium *Candidatus Phytoplasma vitis*, which is transmitted by the insect vector *Scaphoideus titanus* in grapevine crops. The key contribution of this work is the derivation of conditions under which positive periodic solutions exist. These conditions are based on the assumption that key factors such as recruitment rates, disease transmission, and vector infectivity vary periodically, thus reflecting seasonal changes. The existence of these periodic solutions is proven using the degree theory, and numerical examples are provided to support the theoretical findings. This model aims to enhance the understanding of the epidemiological dynamics of flavescence dorée and contribute to developing better control strategies to manage the disease in grapevines.

Keywords: mathematical modeling of plant diseases; periodic solutions in differential equations; disease management in vineyards; seasonal vector population models; vector-borne plant diseases

1. Introduction

1.1. Scope

In recent decades, agricultural exports have become a critical driver of economic growth for many countries, with the wine industry being one of its crucial components [1–5]. It is well-known that

the wine industry, along with businesses and grape agriculture, involves many stakeholders and has attracted diverse perspectives from science and technology. Approaches related to climate change, organic production, and sustainability have increasingly shaped practices in the wine industry [6–8]. Furthermore, vineyards contribute to wine production and serve as a source of income for the tourism sector, thus creating employment and fostering economic development in rural areas where vineyards are located. Overall, vineyards hold a significant role in global agriculture, thereby offering economic, cultural, and social benefits across various regions of the world. These facts underscore the importance of research and innovation to ensure the sustainability of the industry [9, 10]. In this work, we focus specifically on diseases that affect vineyards, as understanding the dynamics of these diseases is crucial for sustainable production and reducing pesticide use, which, in turn, minimizes the environmental impact and production costs [11–15]. Epidemiology, traditionally seen as a descriptive science focused on the ecological factors of diseases, has evolved significantly in recent years. Now, it incorporates more advanced analytical methods, among which mathematical modeling plays a key role [16]. The modeling of infectious disease transmission in human populations has been extensively studied [17–21], and its importance became even more apparent during the COVID-19 pandemic, which highlighted the need for models to inform immediate public health measures [20]. The methodologies used to model human diseases can be generalized to other populations, including animals and plants [16, 19, 22].

A commonly used approach is the compartmental model, which divides the total population into sub-populations (often susceptible, infected, and recovered classes) and uses the laws of interaction and mass conservation to describe the system [23–27]. This methodology can be adapted to model the interaction between two populations, such as animals and plants, to study diseases caused by pathogens such as bacteria, viruses, fungi, and other microscopic organisms [28–33]. In the context of plant diseases, the spread is often modeled through vector-host interactions, where the vector transmits the disease between hosts, as is the case with many vector-borne diseases [28, 29, 34].

In this study, we focus on one such vector-borne disease that affects grapevines: flavescence dorée, that affects caused by the bacterium *Candidatus Phytoplasma vitis* and transmitted by the insect vector *Scaphoideus titanus*. The role of *Scaphoideus titanus* in transmitting flavescence dorée was first proposed in [34], and has since been confirmed in various studies [30]. This leafhopper feeds on the sap of grapevines, acquiring the bacteria from infected plants and transmitting it to healthy ones, thus facilitating the spread of the disease. Flavescence dorée severely impacts the grapevine health and yield, that affects presenting symptoms such as leaf yellowing, stunted growth, and wilting of the grape clusters. Over time, it can also damage the wood tissue of grapevines, thus leading to a significant reduction in grape production.

1.2. Mathematical model for flavescence dorée in grapevines with seasonality

In order to introduce the results of the paper, we first provide the assumptions and the mathematical model. We consider the interaction of two populations: grapevines and vectors, with the total populations denoted by P and V, respectively. The grapevine population is divided into three compartments: P_s, P_e, and P_i, which represent the number of grapevines that are susceptible to infection, exposed to the bacterium via the vector but not yet infective, and infected and infective, respectively. The vector population, denoted by V, is subdivided into three compartments: susceptible, exposed, and infected, denoted by V_s, V_e, and V_i, respectively. We assume that the total grapevine population, $P = P_s + P_e + P_i$, remains constant throughout the epidemic, as grapevines have a much longer life cycle than the vec-

Table 1. Description of variables and parameters in the mathematical model (1.1)–(1.6).

P_s	Number of susceptible grapevines	$(\alpha)^{-1}$	Average incubation time on grapevine
P_e	Number of exposed grapevines	$(\gamma)^{-1}$	Average recovery time of infected grapevines
P_i	Number of infected grapevines	μ	Mortality rate of vectors
V_s	Number of susceptible vectors	$(\theta)^{-1}$	Average incubation time in vector
V_e	Number of Exposed Vectors	$(\kappa)^{-1}$	Average time of vector infection
V_i	Number of infected vectors	$(\nu)^{-1}$	Transmission rate of vectors
Λ	Average insect vector birth rate	P	Total number of grapevines
β	Infection rate of grapevines by vectors	V	Total number of vectors

tors. In contrast, the vector population, $V = V_s + V_e + V_i$, is variable. The dynamics and interactions of these two populations are modeled based on the following assumptions:

(i) The birth and mortality rates of the vectors are given by Λ and $\mu(V) = \mu_1 + \mu_2 V$, respectively, where $(\mu_1)^{-1}$ is the average lifespan of a vector, and $\mu_2 V$ represents the mortality coefficient, which is proportional to the number of vectors. Thus, $V'(t) = \Lambda V - \mu(V)V$ describes the vector population dynamics.

(ii) The infection force from the grapevine to the vector, denoted by Φ_P, is defined as the rate at which the susceptible vectors become infected per unit of time. It is the product of the number of plants N visited by a vector per unit of time, the probability that a plant is infective (P_i/P), and q, which represents the probability of transmission of the bacterium from the plant to the vector. Hence, $\Phi_P = NqP_i/P$, and the number of newly infected vectors per unit of time is given by $\Phi_P V_s = qNV_sP_i/P$.

(iii) The infection force from the vector to the grapevine, denoted by Φ_V, is defined as the rate at which susceptible grapevines are infected per unit of time. It is determined by the number of vectors which visit a plant per unit time, NV/P, the probability that a vector is infective (V_i/V), and q^*, which represents the probability of transmission of the bacterium to the grapevine. Therefore, $\Phi_V = q^*(NV/P)(V_i/V)$, and the number of newly infected grapevines per unit of time is $\Phi_V P_s = q^*NV_iP_s/P$.

(iv) The parameters involved in the dynamics are α, γ, θ, and κ, which represents the rate at which exposed grapevines become infective, the rate at which infected grapevines recover and become susceptible again, the rate at which exposed vectors become infective, and the rate at which infected vectors recover, respectively. We note that $(\alpha)^{-1}$ is the average incubation period of the bacterium in the grapevine, $(\gamma)^{-1}$ is the average infectious period of the grapevine, $(\theta)^{-1}$ is the average incubation period of the bacterium in the vector, and $(\kappa)^{-1}$ is the average recovery time of the vector.

A schematic representation of the model is provided in Figure 1, and a summary of the notation is given in Table 1. Additionally, it is well-established that climate has a significant impact on the population dynamics of insects, which act as carriers for the bacterium *Candidatus Phytoplasma vitis*, which is the causal agent of flavescence dorée disease [11, 35–38]. Consequently, the inclusion of periodicity in the model allows us to account for seasonal variations that affect the spread of the disease, which ultimately leads to more effective and precise strategies to manage grapevine crops. For this

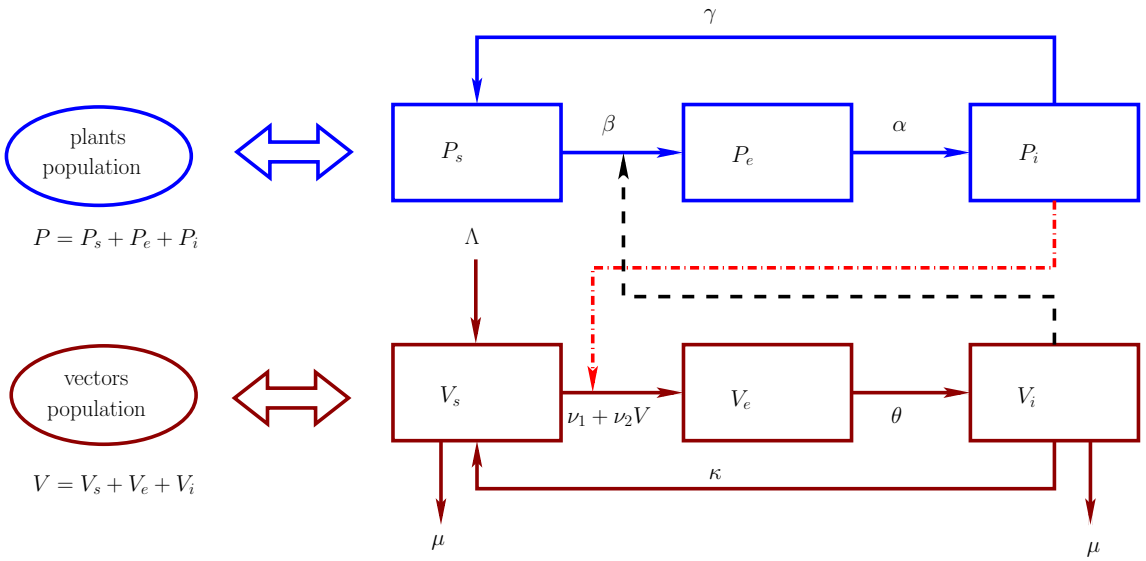

Figure 1. Schematic compartment diagram representation of the propagation of flavescence dorée (vectors) in a grapevine crop (plants).

reason, we assume that the parameters β, α, Λ, ν, θ, μ, and κ vary over time, following a non-negative, ω-periodic pattern.

According to the hypotheses and the previously notation introduced, the dynamics of flavescence dorée propagation in a grapevine population can be modeled by the following system of non-linear differential equations:

$$\frac{dP_s(t)}{dt} = -\beta(t)V_i(t)\frac{P_s(t)}{P} + \gamma(t)P_i(t), \tag{1.1}$$

$$\frac{dP_e(t)}{dt} = \beta(t)V_i(t)\frac{P_s(t)}{P} - \alpha(t)P_e(t), \tag{1.2}$$

$$\frac{dP_i(t)}{dt} = \alpha(t)P_e - \gamma(t)P_i, \tag{1.3}$$

$$\frac{dV_s(t)}{dt} = \Lambda(t)V(t) - \Big(\mu_1(t) + \mu_2(t)V(t)\Big)V_s(t) - \nu(t)V_s(t)\frac{P_i(t)}{P} + \kappa(t)V_i(t), \tag{1.4}$$

$$\frac{dV_e(t)}{dt} = -\Big(\mu_1(t) + \mu_2(t)V(t)\Big)V_e(t) + \nu(t)V_s(t)\frac{P_i(t)}{P} - \theta(t)V_e(t), \tag{1.5}$$

$$\frac{dV_i(t)}{dt} = -\Big(\mu_1(t) + \mu_2(t)V(t)\Big)V_i(t) + \theta(t)V_e(t) - \kappa(t)V_i(t). \tag{1.6}$$

The system (1.1)–(1.6) is supplemented by the following initial conditions:

$$P_s(0) = P_s^0,\ P_e(0) = P_e^0,\ P_i(0) = P_i^0,\ V_s(0) = V_s^0,\ V_e(0) = V_e^0,\ V_e(0) = V_i^0. \tag{1.7}$$

The system (1.1)–(1.6) generalizes the model proposed in [28], where the case with constant coefficients was studied. It is important to note that P is constant, and V satisfies a logistic-type equation with variable coefficients: $V'(t) = \Big[\Lambda(t) - \Big(\mu_1(t) + \mu_2(t)V(t)\Big)\Big]V(t)$.

1.3. Main results of the paper

In this paper, we propose and prove three main results. First, we introduce sufficient conditions for the existence of positive periodic solutions for the model (1.1)–(1.7) (see Theorem 1.1). Second, we establish the existence of a solution for the operator equation (see Theorem 1.2). Finally, we present numerical results to demonstrate the theoretical findings (see Section 5).

We begin by introducing the notation for the space of periodic functions. Specifically, we consider the Banach space E, defined as the space of continuous and ω-periodic functions, defined as the following set:

$$E = \Big\{\mathbf{x} \in C^0(\mathbb{R};\mathbb{R}^6): \quad \mathbf{x}(t+\omega) = \mathbf{x}(t), \qquad \|\mathbf{x}\| := \sum_{i=1}^{6} \max_{t\in[0,\omega]} |x_i(t)| < \infty\Big\}. \tag{1.8}$$

The following theorem provides the result for the existence of positive periodic solutions for the system (1.1)–(1.7):

Theorem 1.1. *Let E the space defined in* (1.8)*. Assume that the initial conditions are positive $\left(P_s^0, P_e^0, P_i^0, V_s^0, V_e^0, V_i^0\right) \in \mathbb{R}_+^6$, and the coefficients $\beta, \alpha, \gamma, \Lambda, \mu_1, \mu_2, \theta, \kappa$, and ν are non-negative $\omega-$periodic functions, with Λ and μ_1 satisfying the relation $(\Lambda - \mu_1)(t) \geq 0$ for $t \in [0, \omega]$. Then, the system* (1.1)–(1.7) *admits at least one $\omega-$periodic solution.*

The methodology used to prove Theorem 1.1 is based on the topological degree theory, specifically Mawhin's Continuation Theorem [39] (see also [40, 41]). Applications of the topological degree theory to epidemiology were recently conducted in [42–44]. If we define $\mathrm{Dom}\,(L) = E \cap C^1(\mathbb{R};\mathbb{R}^6)$ and introduce the the operators L and $N: \mathrm{Dom}\,(L) \subset E \to E$ by the following relations,

$$L(\mathbf{x}) = \left(\frac{d\mathbf{x}}{dt}\right), \tag{1.9}$$

$$\begin{aligned} N(\mathbf{x}) = \Big(& -\beta(t)e^{x_6} + \gamma e^{x_3-x_1}, \quad \beta(t)e^{x_6+x_1-x_2} - \alpha, \quad \alpha e^{x_2-x_3} - \gamma, \\ & \Lambda(t)\Big(e^{x_4} + e^{x_5} + e^{x_6}\Big)e^{-x_4} - \Big(\mu_1 + \mu_2 P\Big(e^{x_4} + e^{x_5} + e^{x_6}\Big)\Big) - \nu(t)e^{x_3} + \kappa e^{x_6-x_4}, \\ & -\Big(\mu_1 + \mu_2 P\Big(e^{x_4} + e^{x_5} + e^{x_6}\Big)\Big) + \nu(t)e^{x_3+x_4-x_5} - \theta, \\ & -\Big(\mu_1 + \mu_2 P\Big(e^{x_4} + e^{x_5} + e^{x_6}\Big)\Big) + \theta e^{x_5-x_6} - \kappa\Big), \end{aligned} \tag{1.10}$$

then we observe that the system (1.1)–(1.7) can be written as the following operator equation:

$$L\mathbf{x} = N\mathbf{x}. \tag{1.11}$$

The rewritten version of (1.1)–(1.7) as the operator equation (1.11) is obtained by introducing $\mathbf{x}(t) = (x_1, \ldots, x_6)(t)$ by the following relation

$$\Big(P_s, P_e, P_i, V_s, V_e, V_i\Big)(t) = \Big(Pe^{x_1(t)}, Pe^{x_2(t)}, Pe^{x_3(t)}, Pe^{x_4(t)}, Pe^{x_5(t)}, Pe^{x_6(t)}\Big). \tag{1.12}$$

More precisely, we have that the following three statements are true: (i) $\mathbf{x}$ is a solution of the operator equation (1.11) if and only if a solution of $\left(P_s, P_e, P_I, V_s, V_e, V_i\right)^T(t)$ is a solution of the system (1.1)–(1.7); (ii) if the solution of (1.11) is $\omega-$periodic, then the solution of system (1.1)–(1.7) is also

$\omega-$periodic; and (iii) if operator equation (1.11) has a solution, the system (1.1)–(1.7) has a positive solution (see Appendix A). Thus, the analysis of the positive periodic solutions of (1.1)–(1.7) is reduced to obtain the existence of solutions of the operator equation (1.11), which will be performed by applying the topological degree theory.

Theorem 1.2. *Consider that the hypotheses of Theorem 1.1 are satisfied, and let L and N be the operators defined in* (1.9) *and* (1.10)*, respectively. Let $\Omega \subset E$ denote the open ball in E centered at $\mathbf{0} \in E$ with radius σ. That is, Ω is the following set:*

$$\Omega = \Big\{\mathbf{x} \in E \ : \ \|\mathbf{x}\| < \sigma\Big\}. \tag{1.13}$$

Then, there exists a solution to the operator equation (1.11)*.*

We note that the radius σ will be defined in terms of the bounds of the coefficients in the mathematical model (1.1)–(1.7).

In the other part of the main results, we consider parameters that arise from experimental data and introduce numerical simulations in which the coefficients are treated as periodic functions.

1.4. Organization of the paper

The article is organized as follows. In Section 2, we recall the definitions and results of Mawhin's degree of coincidence theory, using the framework presented in [39, 40]. In Sections 3 and 4, we present the proofs of Theorems 1.2 and 1.1, respectively. In Section 5, we provide numerical examples. In Section 6, we present the conclusions and outline some directions for future work. Moreover, in Appendix A , we provide the details of the reformulation of the system (1.1)–(1.7) as operator equation, and prove some properties of the operators L and N defined in (1.9) and (1.10), respectively.

2. Preliminaries

In this section, we introduce the notation, terminology, and relevant results of the topological degree theory that are necessary for proving Theorem 1.1 through the application of Mawhin's Continuation Theorem [39–41]. Moreover, we present some properties of operators the L and N defined in (1.9) and (1.10), respectively.

Let us consider X and Z, which are two Banach spaces with norms $\|\cdot\|_X$ and $\|\cdot\|_Y$, respectively; $L : \mathrm{Dom}\,(L) \subset X \to Z$ and $L : X \to Z$ be two operators; and $\Omega \subset E$ be an open bounded set. We assume that L is a linear Fredholm operator of index zero, namely, $\mathrm{Im}\,(L)$ is closed in Z and $\dim(\mathrm{Ker}\,(L)) = \mathrm{codim}(\mathrm{Im}\,(L)) < \infty$. It is well-known that there exists the continuous projectors $P : X \to X$ and $Q : Z \to Z$ such that the following assertions are satisfied

$$\left.\begin{array}{l} \mathrm{Im}\,(P) = \mathrm{Ker}\,(L), \quad \mathrm{Im}\,(L) = \mathrm{Ker}\,(Q) = \mathrm{Im}\,(I-Q), \\ \text{there exists } K_P : \mathrm{Im}\,(L) \to \mathrm{Dom}\,(L) \cap \mathrm{Ker}\,(P) \text{ such that} \\ \qquad\qquad LK_p x = x \text{ for all } x \in \mathrm{Im}\,(L) \text{ and } PK_p = 0, \\ \text{there exists an isomorphism } J : \mathrm{Im}\,(Q) \to \mathrm{Ker}\,(L). \end{array}\right\} \tag{2.1}$$

Meanwhile, we consider that the operator $N : E \to F$ is $L-$compact on $\overline{\Omega}$ (i.e., N is continuous, $QN(\overline{\Omega})$ is bounded, and $K_P(I-Q)N$ is compact on the set $\overline{\Omega}$).

On the other hand, we recall the definition of the degree of a function. Let $U \subset \mathbb{R}^n$ be an open and bounded set, $f : U \to \mathbb{R}^n$ be a given function, and define the set $N_f = \{x \in U : J_f(x) = 0\}$, where $J_f(x)$ denotes the Jacobian of f at x. If $f \in C^1(U, \mathbb{R}^n) \cap C(\overline{U}, \mathbb{R}^n)$ and $y \in \mathbb{R}^n \backslash f(\partial U \cup N_f)$, then

$$\deg\{f, U, y\} = \begin{cases} \sum_{x \in f^{-1}(y)} \operatorname{sgn} J_f(x), & f^{-1}(y) \neq \emptyset, \\ 0, & f^{-1}(y) = \emptyset, \end{cases} \tag{2.2}$$

defines the degree of f on U at y.

The following theorem, often referenced as Mawhin's Continuation Theorem, establishes the specific assemblage of properties of the operators L and N, which are needed to prove the existence of the solution of the operator equation (1.11).

Theorem 2.1. *Assume that X and Y are Banach spaces, $\Omega \subset X$ is and open bounded set, $L : \operatorname{Dom}(L) \subset X \to Y$ is a Fredholm mapping of index zero, and $N : X \to Y$ is a $L-$compact operator on $\overline{\Omega}$. If the following hypotheses are met:*

(C_1) For each $(\lambda, x) \in (0, 1) \times (\partial\Omega \cap \operatorname{Dom}(L))$, the relation $Lx \neq \lambda Nx$ is satisfied.

(C_2) For each $x \in \partial\Omega \cap \operatorname{Ker}(L)$, the relation $QNx \neq 0$ is satisfied.

(C_3) $\deg(JQN, \Omega \cap \operatorname{Ker}(L), 0) \neq 0$.

then there exists at least one $x \in \operatorname{Dom}(L) \cap \overline{\Omega}$ satisfying the operator equation $Lx = Nx$.

Let us consider that $X = Y = F$ and L and N are the operators defined in (1.9) and (1.10). We observe that L and N satisfy the hypotheses of Theorem 2.1. More precisely, we have the following Lemma (for details of the proof see Appendix B).

Lemma 2.1. *Let us consider the operators L and N give by the relations on* (1.9) *and* (1.10)*, respectively, with $X = Y = F$ defined in* (1.8) *and Ω be the set given in* (1.13)*. Then, the following assertions are satisfied*

(a) L is a Fredholm operator of index zero with $\operatorname{Ker} L \cong \mathbb{R}^6$ and $\operatorname{Im}(L) = \left\{\mathbf{y} \in F : \int_0^\omega \mathbf{y}(\tau)d\tau = 0\right\}$.

(b) N is a continuous operator.

(c) Let $\mathbb{P} : F \to F$ defined by $\mathbb{P}(\mathbf{x}) = \omega^{-1} \int_0^\omega \mathbf{x}(\tau)d\tau$. Then, the relations (2.1) *are satisfied if we select $\mathbb{P} = \mathbb{Q}$.*

(d) If the assumptions of Theorem 1.1 are fulfilled, then the operator N is L-compact on $\overline{\Omega}$.

3. Proof of Theorem 1.2

3.1. Some previos results

Hereinafter, we use the notation $\|\cdot\|_\infty$ for $\|\cdot\|_{L^\infty([0,\omega])}$.

Proposition 3.1. *Let L and N be the operators defined in* (1.9) *and* (1.10)*, respectively, and consider the following notation:*

$$\underline{\underline{V}} = \frac{V_s^0 + V_e^0 + V_i^0}{P\Big[\Big(V_s^0 + V_e^0 + V_i^0\Big)\exp\Big(\|\Lambda - \mu_1\|_\infty \omega\Big)\|\mu_2\|_\infty \omega + 1\Big]}, \tag{3.1}$$

$$\overline{\overline{V}} = \frac{V_s^0 + V_e^0 + V_i^0}{P} \exp\Big(\|\Lambda - \mu_1\|_\infty \omega\Big)\|\mu_2\|_\infty \omega. \tag{3.2}$$

If $\lambda \in (0,1)$ *and the assumptions of Theorem 1.1 are satisfied, then the following relations*

$$e^{x_1(t)} + e^{x_2(t)} + e^{x_3(t)} = 1, \quad e^{x_4(t)} + e^{x_5(t)} + e^{x_6(t)} \in [\underline{\underline{V}}, \overline{\overline{V}}], \quad t \in [0, \Omega] \tag{3.3}$$

are satisfied for any $\mathbf{x}$ *solution of the system* $L\mathbf{x}(t) = \lambda N\mathbf{x}(t)$.

Proof. In order to prove (3.3), we multiply each equation of the system $L\mathbf{x}(t) = \lambda N\mathbf{x}(t)$ by $e^{x_i(t)}$; by regrouping and adding the resulting equations, we deduce the following

$$\frac{d}{dt}\Big(e^{x_1} + e^{x_2} + e^{x_3}\Big) = 0, \tag{3.4}$$

$$\frac{d}{dt}\Big(e^{x_4} + e^{x_5} + e^{x_6}\Big) = \lambda(\Lambda - \mu_1)(t)\Big(e^{x_4} + e^{x_5} + e^{x_6}\Big) - \lambda\mu_2(t)P\Big(e^{x_4} + e^{x_5} + e^{x_6}\Big)^2. \tag{3.5}$$

From (3.4) and the integration on $[0, t]$, we deduce the first relation in (3.3), since

$$e^{x_1(t)} + e^{x_2(t)} + e^{x_3(t)} = e^{x_1(0)} + e^{x_2(0)} + e^{x_3(0)} = \frac{P_s^0}{P} + \frac{P_e^0}{P} + \frac{P_i^0}{P} = \frac{P_s^0 + P_e^0 + P_i^0}{P} = 1.$$

Similarly, by integration of (3.5) as a Bernoulli equation, we obtain the following

$$\begin{aligned} e^{x_4(t)} + e^{x_5(t)} + e^{x_6(t)} &= \frac{\Big(e^{x_4(0)} + e^{x_5(0)} + e^{x_6(0)}\Big)\exp\Big(\int_0^t \lambda(\Lambda - \mu_1)(s)ds\Big)}{\Big(e^{x_4(0)} + e^{x_5(0)} + e^{x_6(0)}\Big)P\lambda\int_0^t \exp\Big(\int_0^s \lambda(\Lambda - \mu_1)(\tau)d\tau\Big)\mu_2(s)ds + 1} \\ &= \frac{\Big(V_s^0 + V_e^0 + V_i^0\Big)\exp\Big(\int_0^t \lambda(\Lambda - \mu_1)(s)ds\Big)}{P\left[\Big(V_s^0 + V_e^0 + V_i^0\Big)\lambda\int_0^t \exp\Big(\int_0^s \lambda(\Lambda - \mu_1)(\tau)d\tau\Big)\mu_2(s)ds + 1\right]}. \end{aligned} \tag{3.6}$$

From the hypothesis of Theorem 1.1, we have that $0 \leq \min_{t\in[0,\omega]} \lambda(\Lambda - \mu_1)(t) \leq \lambda(\Lambda - \mu_1)(t) \leq \|\Lambda - \mu_1\|_\infty$ for $t \in [0, \omega]$. Then, using the increasing behavior of the exponential function and the fact that $\lambda \in (0,1)$, we obtain the following inequality:

$$1 \leq \exp\Big(\min_{t\in[0,\omega]} \lambda(\Lambda - \mu_1)(t)\Big) \leq \exp\Big(\int_0^t \lambda(\Lambda - \mu_1)(s)ds\Big) \leq \exp\Big(\|\Lambda - \mu_1\|_\infty \omega\Big), \quad t \in [0, \omega]. \tag{3.7}$$

Considering s instead of t in the upper limit of the integral given on the estimate (3.7), and multiplying by $\mu_2(s)$ and integrating on $[0, t] \subset [0, \omega]$, we deduce the following:

$$\begin{aligned} 0 \leq t \min_{t\in[0,\omega]} \mu_2(t) \leq t \min_{t\in[0,\omega]} \mu_2(t) \exp\Big(\min_{t\in[0,\omega]} \lambda(\Lambda - \mu_1)(t)\Big) &\leq \lambda \int_0^t \exp\Big(\int_0^s \lambda(\Lambda - \mu_1)(\tau)d\tau\Big)\mu_2(s)ds \\ &\leq \exp\Big(\|\Lambda - \mu_1\|_\infty \omega\Big)\|\mu_2\|_\infty \omega, \quad t \in [0, \omega], \end{aligned}$$

which implies the following estimates

$$\begin{aligned} 1 &\leq \Big(V_s^0 + V_e^0 + V_i^0\Big)\lambda\int_0^t \exp\Big(\int_0^s \lambda(\Lambda - \mu_1)(\tau)d\tau\Big)\mu_2(s)ds + 1 \\ &\leq \Big(V_s^0 + V_e^0 + V_i^0\Big)\exp\Big(\|\Lambda - \mu_1\|_\infty \omega\Big)\|\mu_2\|_\infty \omega + 1, \quad t \in [0, \omega]. \end{aligned} \tag{3.8}$$

From (3.7) and (3.8) in (3.6), we deduce the second relation in (3.3).

Proposition 3.2. *[42] Let $\Psi : [0,\omega] \subset \mathbb{R}^+ \to \mathbb{R}$ be a function such that is absolutely continuous and satisfies the following differential inequality:*

$$\frac{d}{dt}\Psi(t) + m(t)\Psi(t) \geq 0, \quad \forall t \in [0,\omega], \tag{3.9}$$

for a function $m \in L^1([0,\omega])$ which is bounded on $[0,\omega]$ (i.e., there exists $m_1, m_2 \in \mathbb{R}_+$ such that $0 < m_1 \leq m(t) \leq m_2$ for all $t \in [0,\omega]$). Then, the assumption $\Psi(0) > 0$ implies the estimate $\Psi(t) \geq \Psi(0)\exp(-m_2\omega) > 0$ for all $t \in [0,\omega]$.

3.2. A priori estimates

Lemma 3.1. *Assume that the hypotheses of Lemma 2.1 and Theorem 1.1 are satisfied. Additionally, if $(\lambda, \mathbf{x}) \in (0,1) \times (\partial\Omega \cap \mathrm{Dom}(L))$ is a solution of the operator equation $L\mathbf{x} = \lambda N\mathbf{x}$. Then, there exist the positive constants ρ_k, d_k, and δ_k such that the following inequalities*

$$0 < \ln(\delta_k) < x_k(t) < \ln\left(\frac{\rho_k}{\omega}\right) + d_k, \quad k = \overline{1,6}, \tag{3.10}$$

are satisfied for $t \in [0,\omega]$.

Proof. The proof is constructive. First we find the definition of the constant δ_k, and subsequently the constants $\rho_k$and d_k. In order to obtain δ_k, we arbitrarily chose $\mathbf{x} \in \mathrm{Dom}(L)$ such that $L\mathbf{x} = \lambda N\mathbf{x}$. By multiplying each equation of the system $(L\mathbf{x})^T(t) = \lambda(N\mathbf{x})^T(t)$ and rearranging the result appropriately, we deduce the following:

$$\frac{de^{x_1}}{dt} + \Big[\lambda\beta(t)e^{x_6}\Big]e^{x_1} = \lambda\gamma(t)e^{x_3} > 0, \tag{3.11}$$

$$\frac{de^{x_2}}{dt} + \lambda\alpha(t)e^{x_2} = \lambda\beta(t)e^{x_6+x_1} > 0, \tag{3.12}$$

$$\frac{de^{x_3}}{dt} + \lambda\gamma(t)e^{x_3} = \lambda\alpha(t)e^{x_2} > 0, \tag{3.13}$$

$$\frac{de^{x_4}}{dt} + \Big[\lambda\Big(\mu_1(t) + \mu_2(t)P\Big(e^{x_4} + e^{x_5} + e^{x_6}\Big)\Big) + \lambda\nu(t)e^{x_3}\Big]e^{x_4} = \lambda\Lambda(t)\Big(e^{x_4} + e^{x_5} + e^{x_6}\Big) + \lambda\kappa e^{x_6} > 0, \tag{3.14}$$

$$\frac{de^{x_5}}{dt} + \Big[\lambda\Big(\mu_1(t) + \mu_2(t)P\Big(e^{x_4} + e^{x_5} + e^{x_6}\Big)\Big) + \lambda\theta(t)\Big]e^{x_5} = \lambda\nu(t)e^{x_3+x_4} > 0, \tag{3.15}$$

$$\frac{de^{x_6}}{dt} + \Big[\lambda\Big(\mu_1(t) + \mu_2(t)P\Big(e^{x_4} + e^{x_5} + e^{x_6}\Big)\Big) + \lambda\kappa(t)\Big]e^{x_6} = \lambda\theta(t)e^{x_5} > 0. \tag{3.16}$$

From the estimates in (3.3) and the assumptions of Theorem 1.1, we have the following inequalities

$$\begin{aligned}
0 < \min_{t\in[0,\omega]}\Big[\lambda\Big(\mu(t) + \mu_2(t)P\underline{V}\Big) + \lambda\theta(t)\Big] &\leq \lambda\Big(\mu_1(t) + \mu_2(t)P\Big(e^{x_4} + e^{x_5} + e^{x_6}\Big)\Big) + \lambda\theta(t) \\
&\leq \|\mu_1\|_\infty + \|\mu_2\|_\infty P\overline{\overline{V}} + \|\theta\|_\infty, \quad t \in [0,\omega], \\
0 < \min_{t\in[0,\omega]}\Big[\lambda\Big(\mu_1(t)\mu_2(t)P\underline{V}\Big) + \lambda\kappa(t)\Big] &\leq \lambda\Big(\mu_1(t) + \mu_2(t)P\Big(e^{x_4} + e^{x_5} + e^{x_6}\Big)\Big) + \lambda\kappa(t) \\
&\leq \|\mu_1\|_\infty + \|\mu_2\|_\infty P\overline{\overline{V}} + \|\kappa\|_\infty, \quad t \in [0,\omega].
\end{aligned}$$

By using the fact that $e^{x_5(0)} = V_e^0/P$ and $e^{x_6(0)} = V_i^0/P$, and applying Proposition 3.2 to (3.15) and (3.16), we deduce the following estimates:

$$e^{x_5(t)} \geq \frac{V_e^0}{P} \exp\Big(- \Big[||\mu_1||_\infty + ||\mu_2||_\infty P\overline{\overline{V}} + ||\theta||_\infty\Big]\omega\Big) := \delta_5, \quad t \in [0, \omega], \tag{3.17}$$

$$e^{x_6(t)} \geq \frac{V_i^0}{P} \exp\Big(- \Big[||\mu_1||_\infty + ||\mu_2||_\infty P\overline{\overline{V}} + ||\kappa||_\infty\Big]\omega\Big) := \delta_6, \quad t \in [0, \omega]. \tag{3.18}$$

We notice that (3.3) and (3.18) imply the following inequalities:

$$\begin{aligned}
&0 < \min_{t\in[0,\omega]} \Big[\lambda\beta(t)\Big]\delta_6 \leq \lambda\beta(t)e^{x_6(t)} \leq ||\beta||_\infty \overline{\overline{V}}, \quad t \in [0, \omega],\\
&0 < \lambda \min_{t\in[0,\omega]} \alpha(t) \leq \lambda\alpha(t) \leq ||\alpha||_\infty, \quad t \in [0, \omega],\\
&0 < \lambda \min_{t\in[0,\omega]} \gamma(t) \leq \lambda\gamma(t) \leq ||\gamma||_\infty, \quad t \in [0, \omega].
\end{aligned}$$

Then, the application of Proposition 3.2 to (3.11), (3.12), and (3.13) implies the following:

$$e^{x_1(t)} > e^{x_1(0)} \exp\Big(- ||\beta||_\infty \overline{\overline{V}}\omega\Big) = \frac{P_s^0}{P} \exp\Big(- ||\beta||_\infty \overline{\overline{V}}\omega\Big) := \delta_1, \quad t \in [0, \omega], \tag{3.19}$$

$$e^{x_2(t)} > e^{x_2(0)} \exp\Big(- ||\alpha||_\infty\omega\Big) = \frac{P_e^0}{P} \exp\Big(- ||\alpha||_\infty\omega\Big) := \delta_2, \quad t \in [0, \omega], \tag{3.20}$$

$$e^{x_3(t)} > e^{x_3(0)} \exp\Big(- ||\gamma||_\infty\omega\Big) = \frac{P_i^0}{P} \exp\Big(- ||\gamma||_\infty \overline{\overline{V}}\omega\Big) := \delta_3, \quad t \in [0, \omega]. \tag{3.21}$$

Similarly, from (3.3) and (3.21), we deduce the following:

$$\begin{aligned}
0 &< \min_{t\in[0,\omega]} \Big[\lambda\Big(\mu_1(t) + \mu_2(t)P\underline{\underline{V}}\Big) + \lambda\nu(t)\delta_3\Big]\\
&\leq \lambda\Big[\mu_1(t) + \mu_2(t)P\Big(e^{x_4(t)} + e^{x_5(t)} + e^{x_6(t)}\Big)\Big] + \lambda\nu(t)e^{x_3(t)}\\
&\leq ||\mu_1||_\infty + ||\mu_2||_\infty P\overline{\overline{V}} + ||\nu||_\infty, \quad t \in [0, \omega],
\end{aligned}$$

and by the initial condition $e^{x_4(0)} = V_s^0/P$ and Proposition 3.2, we obtain the following:

$$e^{x_4(t)} > \frac{V_s^0}{P} \exp\Big(- ||\beta||_\infty\Big[||\mu_1||_\infty + ||\mu_2||_\infty P\overline{\overline{V}} + ||\nu||_\infty\Big]\omega\Big) := \delta_4, \quad t \in [0, \omega]. \tag{3.22}$$

The relations (3.17)–(3.22) prove the following estimate:

$$0 < \ln(\delta_k) < x_k(t), \quad k = 1, \ldots, 6, \quad t \in [0, \omega]. \tag{3.23}$$

The construction of ρ_k for any $\mathbf{x} \in \text{Dom}\,(L)$ which satisfies the operator equation $L\mathbf{x} = \lambda N\mathbf{x}$ can be developed as follows. From Proposition 3.1, we deduce that the following:

$$0 < \int_0^\omega (e^{x_k})\, dt \leq \int_0^\omega \Big(e^{x_1(t)} + e^{x_2(t)} + e^{x_3(t)}\Big)\, dt = \int_0^\omega dt = \omega := \rho_k, \quad k = 1, 2, 3, \tag{3.24}$$

$$0 < \int_0^\omega (e^{x_\ell})\, dt \leq \int_0^\omega \Big(e^{x_4(t)} + e^{x_5(t)} + e^{x_6(t)}\Big)\, dt = \int_0^\omega \overline{\overline{V}} dt = \overline{\overline{V}}\omega := \rho_\ell, \quad \ell = 4, 5, 6. \tag{3.25}$$

Applying the Mean Value Theorem for integrals to the function e^{x_k} for $k = 1, \ldots, 6$ over $[0, \omega]$, we follow that there exists $\xi_k \in [0, \omega]$ such that $e^{x_k(\xi_k)} = \omega^{-1} \int_0^\omega e^{x_k} dt$, and consequently

$$\text{there exists } \xi_k \in [0, \omega] \text{ such that } x_k(\xi_k) = \ln\left(\frac{\rho_k}{\omega}\right), \quad k = 1, \ldots, 6. \tag{3.26}$$

Integrating the system $(L\mathbf{x})^T(t) = \lambda(N\mathbf{x})^T(t)$ over $[0, \omega]$ and the $\omega-$periodic behavior of $\mathbf{x}$, we obtain the following:

$$\begin{aligned}
&\int_0^\omega \lambda\left(-\beta e^{x_6} + \gamma e^{x_3 - x_1}\right) dt = 0, \qquad \int_0^\omega \lambda\left(\beta e^{x_1 + x_6 - x_2} - \alpha\right) dt = 0, \qquad \int_0^\omega \lambda\left(\alpha e^{x_2 - x_3} - \gamma\right) dt = 0,\\
&\int_0^\omega \lambda\Big(\Lambda\Big(e^{x_4} + e^{x_5} + e^{x_6}\Big)e^{-x_4} - \Big(\mu_1 + \mu_2 P\Big(e^{x_4} + e^{x_5} + e^{x_6}\Big)\Big) - \nu(t)e^{x_3} + \kappa(t)e^{x_6 - x_4}\Big) dt = 0,\\
&\int_0^\omega \lambda\Big(-\Big(\mu_1 + \mu_2 P\Big(e^{x_4} + e^{x_5} + e^{x_6}\Big)\Big) + \nu e^{x_3 + x_4 - x_5} - \theta(t)\Big) dt = 0,\\
&\int_0^\omega \lambda\Big(-\Big(\mu_1 + \mu_2 P\Big(e^{x_4} + e^{x_5} + e^{x_6}\Big)\Big) + \theta(t)e^{x_5 - x_6} - \kappa(t)\Big) dt = 0,
\end{aligned}$$

which implies that

$$\begin{aligned}
&\int_0^\omega e^{(x_3 - x_1)(t)} dt \le \frac{\|\beta\|_\infty \overline{\overline{V}}\omega}{\min_{t\in[0,\omega]} \gamma(t)}, && \int_0^\omega e^{(x_1 + x_6 - x_2)(t)} dt \le \frac{\|\alpha\|_\infty \omega}{\min_{t\in[0,\omega]} \beta(t)},\\
&\int_0^\omega e^{(x_2 - x_3)(t)} dt \le \frac{\|\gamma\|_\infty \omega}{\min_{t\in[0,\omega]} \alpha(t)}, && \int_0^\omega e^{-x_4(t)} dt \le \frac{\Big(\|\mu_1\|_\infty + \|\mu_2\|_\infty P\overline{\overline{V}} + \|\nu\|_\infty\Big)\omega}{\underline{\underline{V}} \min_{t\in[0,\omega]} \Lambda(t)},\\
&\int_0^\omega e^{(x_6 - x_4)(t)} dt \le \frac{\Big(\|\mu_1\|_\infty + \|\mu_2\|_\infty P\overline{\overline{V}} + \|\nu\|_\infty\Big)\omega}{\min_{t\in[0,\omega]} \kappa(t)}, && \int_0^\omega e^{(x_4 + x_3 - x_5)(t)} dt \le \frac{\Big(\|\mu_1\|_\infty + \|\mu_2\|_\infty P\overline{\overline{V}} + \|\theta\|_\infty\Big)\omega}{\min_{t\in[0,\omega]} \nu(t)},\\
&\int_0^\omega e^{(x_5 - x_6)(t)} dt \le \frac{\Big(\|\mu_1\|_\infty + \|\mu_2\|_\infty P\overline{\overline{V}} + \|\kappa\|_\infty\Big)\omega}{\min_{t\in[0,\omega]} \theta(t)}.
\end{aligned}$$

Then, taking the absolute value of the system $(L\mathbf{x})^T(t) = \lambda(N\mathbf{x})^T(t)$ and integrating over $[0, \omega]$, we obtain the following upper bounds:

$$\int_0^\omega \left|\frac{dx_1}{dt}\right| dt \le \int_0^\omega \Big(\beta e^{x_6} + \gamma e^{x_3 - x_1}\Big)(t) dt \le \|\beta\|_\infty \overline{\overline{V}}\omega\left(1 + \frac{\|\gamma\|_\infty}{\min_{t\in[0,\omega]} \gamma(t)}\right) := d_1, \tag{3.27}$$

$$\int_0^\omega \left|\frac{dx_2}{dt}\right| dt \le \int_0^\omega \Big(\beta e^{x_6 + x_1 + x_2} + \alpha\Big)(t) dt \le \|\alpha\|_\infty \omega\left(1 + \frac{\|\beta\|_\infty}{\min_{t\in[0,\omega]} \beta(t)}\right) := d_2, \tag{3.28}$$

$$\int_0^\omega \left|\frac{dx_3}{dt}\right| dt \le \int_0^\omega \Big(\alpha e^{x_2 - x_3} + \gamma\Big)(t) dt \le \|\gamma\|_\infty \omega\left(1 + \frac{\|\alpha\|_\infty}{\min_{t\in[0,\omega]} \alpha(t)}\right) := d_3, \tag{3.29}$$

$$\begin{aligned}
\int_0^\omega \left|\frac{dx_4}{dt}\right| dt &\le \int_0^\omega \Big[\Lambda\Big(e^{x_4} + e^{x_5} + e^{x_6}\Big)e^{-x_4} + \Big(\mu_1 + \mu_2 P\Big(e^{x_4} + e^{x_5} + e^{x_6}\Big)\Big) + \nu e^{x_3} + \kappa e^{x_6 - x_4}\Big](t) dt\\
&\le \omega\Big(\|\mu_1\|_\infty + \|\mu_2\|_\infty P\overline{\overline{V}} + \|\nu\|_\infty\Big)\left(1 + \frac{\overline{\overline{V}}\|\Lambda\|_\infty}{\underline{\underline{V}} \min_{t\in[0,\omega]} \Lambda(t)} + \frac{\|\kappa\|_\infty}{\min_{t\in[0,\omega]} \kappa(t)}\right) := d_4,
\end{aligned} \tag{3.30}$$

$$\int_0^\omega \left|\frac{dx_5}{dt}\right| dt \le \int_0^\omega \left[\left(\mu_1 + \mu_2 P\left(e^{x_4} + e^{x_5} + e^{x_6}\right)\right) + \nu e^{x_4+x_3-x_5} + \theta\right](t)dt$$
$$\le \omega\left(\|\mu_1\|_\infty + \|\mu_2\|_\infty P\overline{\overline{V}} + \|\theta\|_\infty\right)\left(1 + \frac{\|\nu\|_\infty}{\min_{t\in[0,\omega]}\nu(t)}\right) := d_5, \tag{3.31}$$
$$\int_0^\omega \left|\frac{dx_6}{dt}\right| dt \le \int_0^\omega \left[\left(\mu_1 + \mu_2 P\left(e^{x_4} + e^{x_5} + e^{x_6}\right)\right) + \theta e^{x_5-x_6} + \kappa\right](t)dt$$
$$\le \omega\left(\|\mu_1\|_\infty + \|\mu_2\|_\infty P\overline{\overline{V}} + \|\kappa\|_\infty\right)\omega\left(1 + \frac{\|\theta\|_\infty}{\min_{t\in[0,\omega]}\theta(t)}\right) := d_6. \tag{3.32}$$

To complete the proof, we note $\int_{\xi_k}^t x_k'(\tau)d\tau = x_k(t) - x_k(\xi_k)$ for $k = 1, \ldots, 6$. Then, from (3.26) and (3.27)–(3.32), we have the following:

$$x_k(t) = x_k(\xi_k) + \int_{\xi_k}^t \frac{dx_k(\tau)}{d\tau}d\tau$$
$$\le x_k(\xi_k) + \int_0^\omega \left|\frac{dx_k(\tau)}{d\tau}\right| d\tau \le \ln\left(\frac{\rho_k}{\omega}\right) + d_k, \quad k = 1, \ldots, 6, \quad t \in [0, \omega]. \tag{3.33}$$

Hence, by the estimates (3.23) and (3.33), we deduce (3.34) and conclude the proof of the lemma.

Lemma 3.2. *Assume that the hypotheses of Lemma 3.1 are satisfied. If* $\mathbf{x} \in \text{Ker}\,(L)$ *is a solution of the operator equation* $\mathbb{Q}N(\mathbf{x}) = 0$*, then there exist positive constants* ρ_k *and* δ_k *such that the inequality*

$$0 < \ln(\delta_k) < x_k(t) < \ln(\frac{\rho_k}{\omega}), \quad k = 1, \ldots, 6, \tag{3.34}$$

is satisfied for $t \in [0, \omega]$.

Proof. From Lemma 2.1, it follows that $Ker(L) \cong \mathbb{R}^6$, which implies that $\mathbf{x} \in \text{Ker}\,(L)$ is equivalent to $\mathbf{x} = \mathbf{c}$, where $\mathbf{c}$ is a constant vector. Assume the hypothesis that $\mathbf{x}$ satisfies the operator equation $\mathbb{Q}N(\mathbf{x}) = \mathbf{0}$, or equivalently $\mathbb{Q}N(\mathbf{c}) = \mathbf{0}$. From the definition of $\mathbb{Q}$, we follow that

$$\mathbb{Q}N(\mathbf{c}) = \mathbf{0} \quad \Leftrightarrow \quad \frac{1}{\omega}\int_0^\omega N(\mathbf{c})d\tau = \mathbf{0} \quad \Leftrightarrow \quad N(\mathbf{c}) = \mathbf{0} = L(\mathbf{c}).$$

Then, for any $\lambda \in (0, 1)$, it follows that $\lambda N(\mathbf{c}) = \mathbf{0} = L(\mathbf{c})$ and consequently $\lambda N(\mathbf{c}) = L(\mathbf{c})$. Then, by similar arguments to the proof of Lemma 3.1, we deduce there exist δ_k, ρ_k and $d_k = 0$ for $k = 1, \ldots, 6$ such that the estimate (3.34) is satisfied.

Lemma 3.3. *Let* $X = Y = F$ *with* F*, the Banach spaces are defined in* (1.8)*;* $\Omega \subset F$*, the open ball centred at* $\mathbf{0}$ *and radius* h*, with* h *defined as follows:*

$$h = \max\left\{\sum_{k=1}^6 \ln(\delta_k); \sum_{k=1}^6 \left(\ln(\frac{\rho_k}{\omega}) + d_k\right)\right\} \tag{3.35}$$

where δ_k, ρ_k*, and* d_k *are as defined in* (3.19) *and* (3.20)*,* (3.24) *and* (3.25)*, and* (3.27)–(3.32)*, respectively. Then, the items (C1), (C2), and (C3) of Theorem 2.1 are satisfied.*

Proof. The proof of (C1) will be developed by contradiction. We begin by considering that the statement is false, or equivalently we consider that there exists $(\lambda, \mathbf{x}) \in (0,1) \times [\partial\Omega \cap \text{Dom}\,(L)]$ such that $L(\mathbf{x}) = \lambda N(\mathbf{x})$. Then, by the application of Lemma 3.1, we follow that $0 < \ln(\delta_k) < x_k(t) < \ln(\rho_k/\omega) + d_k$ for $k = 1, \ldots, 6$, which implies the following:

$$\sum_{k=1}^{6} \ln(\delta_k) < \sum_{k=1}^{6} x_k(t) < \sum_{k=1}^{6} \left(\ln\left(\frac{\rho_k}{\omega}\right) + d_k \right), \quad t \in [0, \omega]. \tag{3.36}$$

Using the definition of h given on (3.35), we have that that h can reduced to the following relation:

$$h = \max\left\{ \sum_{k=1}^{6} \ln(\delta_k); \sum_{k=1}^{6} \left(\ln(\frac{\rho_k}{\omega}) + d_k \right) \right\} = \sum_{k=1}^{6} \left(\ln\left(\frac{\rho_k}{\omega}\right) + d_k \right).$$

We notice that (3.36) implies the relation $\|\mathbf{x}\| < h$, or equivalently $\mathbf{x}$ belongs to the interior of Ω, which is a contradiction, since we have assumed that $\mathbf{x} \in \partial\Omega$.

To prove (C2), we also apply a contradiction argument. If (C2) is false, then we can find $\mathbf{x} \in \text{Ker}\,(L) \cap \partial\Omega$, such that $\mathbb{Q}N(\mathbf{x}) = 0$. Then, by Lemma (3.2), we follow that $0 < \ln(\delta_k) < x_k(t) < \ln(\rho_k/\omega)$ for $k = 1, \ldots, 6$, and consequently

$$h = \max\left\{ \sum_{k=1}^{6} \ln(\delta_k); \sum_{k=1}^{6} \ln(\rho_k) \right\} = \sum_{k=1}^{6} \ln\left(\frac{\rho_k}{\omega}\right) \quad \text{and} \quad \|\mathbf{x}\| < h.$$

Here, $\mathbf{x} \in \Omega$ is a contradiction, since we have considered that $\mathbf{x} \in \text{Ker}\,(L) \cap \partial\Omega$. Then, (C2) is satisfied.

In order to prove (C3), we consider $\mathbf{x} \in \text{Dom}\,(L)$ and $\varepsilon \in [0,1]$, and define the homotopy $H : \text{Dom}\,(L) \times [0,1] \to E$, by the following relation:

$$H(\mathbf{x}, \varepsilon) = \begin{pmatrix} -\overline{\beta}e^{x_6} + \overline{\gamma} \\ \overline{\beta}e^{x_6 + x_1 - x_2} - \overline{\alpha} \\ \overline{\alpha}e^{x_2 - x_3} - \overline{\gamma} \\ \overline{\kappa}e^{x_6 - x_4} - \overline{\mu}_1 \\ \overline{\nu}e^{x_4 + x_3 - x_5} - (\overline{\mu}_1 + \overline{\theta}) \\ \overline{\theta}e^{x_5 - x_6} - (\overline{\mu}_1 + \overline{\kappa}) \end{pmatrix}^T + \varepsilon \begin{pmatrix} \overline{\gamma}\left(e^{x_3 - x_1} - 1\right) \\ 0 \\ 0 \\ \overline{\Lambda}\left(e^{x_4} + e^{x_5} + e^{x_6}\right)e^{-x_4} - \overline{\mu}_2 P\left(e^{x_4} + e^{x_5} + e^{x_6}\right) - \overline{\nu}e^{x_3} \\ -\overline{\mu}_2 P\left(e^{x_4} + e^{x_5} + e^{x_6}\right) \\ -\overline{\mu}_2 P\left(e^{x_4} + e^{x_5} + e^{x_6}\right) \end{pmatrix}^T,$$

where

$$\left(\overline{\beta}, \overline{\alpha}, \overline{\gamma}, \overline{\kappa}, \overline{\nu}, \overline{\theta}, \overline{\Lambda}, \overline{\mu_1}, \overline{\mu_2}\right) = \frac{1}{\omega} \int_0^{\omega} \left(\beta, \alpha, \gamma, \kappa, \nu, \theta, \Lambda, \mu_1, \mu_2\right)(t)dt.$$

We claim the following:

$$\text{If } \mathbf{x} \in \text{Ker}\,(L) \cap \partial\Omega \text{ and } \varepsilon \in [0,1], \text{ then } H(\mathbf{x}, \varepsilon) \neq 0. \tag{3.37}$$

Indeed, suppose that there exists $\mathbf{x} \in \text{Ker}\,(L) \cap \partial\Omega$ and $\varepsilon \in [0,1]$ such that $H(\mathbf{x}, \varepsilon) = 0$. Since $\text{Ker}\,(L) \cong \mathbb{R}^6$, we have that $\mathbf{x}(t) = \mathbf{x}(0)$ and $H(\mathbf{x}, \varepsilon) = H(\mathbf{x}(0), \varepsilon) = 0$. Therefore, from the definition of H,

$$0 = -\overline{\beta}e^{x_6(0)} + \overline{\gamma} + \varepsilon\overline{\gamma}\left(e^{x_3 - x_1} - 1\right)$$

$$
\begin{aligned}
0 &= \overline{\beta}e^{(x_1+x_6-x_2)(0)} - \overline{\alpha},\\
0 &= \overline{\alpha}e^{(x_2-x_3)(0)} - \overline{\gamma},\\
0 &= \overline{\kappa}e^{(x_6-x_4)(0)} - \overline{\mu}_1 + \varepsilon\Big[\overline{\Lambda}\Big(e^{x_4(0)} + e^{x_5(0)} + e^{x_6(0)}\Big)e^{-x_4(0)} - \overline{\mu}_2 P\Big(e^{x_4(0)} + e^{x_5(0)} + e^{x_6(0)}\Big) - \overline{\nu}e^{x_3(0)}\Big],\\
0 &= \overline{\nu}e^{(x_3+x_4-x_5)(0)} - (\overline{\mu}_1 + \overline{\theta}) - \varepsilon\overline{\mu}_2 P\Big(e^{x_4(0)} + e^{x_5(0)} + e^{x_6(0)}\Big),\\
0 &= \overline{\theta}e^{(x_5-x_6)(0)} - (\overline{\mu}_1 + \overline{\kappa}) - \varepsilon\overline{\mu}_2 P\Big(e^{x_4(0)} + e^{x_5(0)} + e^{x_6(0)}\Big).
\end{aligned}
$$

Proceeding analogously to the proof of Lemma 3.1, we can deduce that $\|\mathbf{x}(0)\| < h$, or equivalently $\mathbf{x}(t) = \mathbf{x}(0) \in \Omega$, which is a contradiction with the assumption that $\mathbf{x} \in \partial\Omega$. Hence, the claim (3.37) is verified.

On the other hand, it is known that there exists an isomorphism $J : \mathrm{Ker}\,(L) \to \mathrm{Im}\,(\mathbb{Q})$, which implies that $\mathrm{Ker}\,(L) \cong \mathrm{Im}\,(\mathbb{Q})$. Then, without a loss of generality, we can choose $J = I$. It follows that: $J\mathbb{Q}N = I\mathbb{Q}N = \mathbb{Q}N$ and $\deg(J\mathbb{Q}N(\mathbf{x}),\ \mathrm{Ker}\,(L) \cap \Omega,\ \mathbf{0}) = \deg(\mathbb{Q}N(\mathbf{x}),\ \mathrm{Ker}\,(L) \cap \Omega,\ \mathbf{0})$. Then, from (3.37), we can use the homotopy invariance property of the degree of coincidence to obtain the following:

$$
\deg(\mathbb{Q}N(\mathbf{x}),\ \mathrm{Ker}\,(L) \cap \Omega,\ \mathbf{0}) = \deg(H(\mathbf{x}, 1),\ \mathrm{Ker}\,(L) \cap \Omega,\ \mathbf{0}) = \deg(H(\mathbf{x}, 0),\ \mathrm{Ker}\,(L) \cap \Omega,\ \mathbf{0}).
$$

Using the facts that

$$
H(\mathbf{x}, 0) = \Big(-\overline{\beta}e^{x_6} + \overline{\gamma}, \overline{\beta}e^{x_1+x_6-x_2} - \overline{\alpha}, \overline{\alpha}e^{x_2-x_3} - \overline{\gamma}, \overline{\kappa}e^{x_6-x_4} - \overline{\mu}_1, \overline{\nu}e^{x_3+x_4-x_5} - (\overline{\mu}_1 + \overline{\theta}), \overline{\theta}e^{x_5-x_6} - (\overline{\mu}_1 + \overline{\kappa})\Big),
$$

and the algebraic system $H(\mathbf{x}, 0) = 0$, i.e.,

$$
\begin{aligned}
0 &= -\overline{\beta}e^{x_6} + \overline{\gamma},\\
0 &= \overline{\beta}e^{x_1+x_6-x_2} - \overline{\alpha},\\
0 &= \overline{\alpha}e^{x_2-x_3} - \overline{\gamma},\\
0 &= \overline{\kappa}e^{x_6-x_4} - \overline{\mu}_1,\\
0 &= \overline{\nu}e^{x_3+x_4-x_5} - (\overline{\mu}_1 + \overline{\theta}),\\
0 &= \overline{\theta}e^{x_5-x_6} - (\overline{\mu}_1 + \overline{\kappa}),
\end{aligned}
$$

has a unique solution $\mathbf{x}^* \in \partial\Omega \cap \mathrm{Ker}\,(L)$, we deduce the following:

$$
\begin{aligned}
&\deg(H(\mathbf{x}, 0),\ \mathrm{Ker}\,(L) \cap \Omega,\ \mathbf{0})\\
&= \mathrm{sgn}\begin{pmatrix}
\partial_{x1}H_1(\mathbf{x}^*,0) & \partial_{x2}H_1(\mathbf{x}^*,0) & \partial_{x3}H_1(\mathbf{x}^*,0) & \partial_{x4}H_1(\mathbf{x}^*,0) & \partial_{x5}H_1(\mathbf{x}^*,0) & \partial_{x6}H_1(\mathbf{x}^*,0)\\
\partial_{x1}H_2(\mathbf{x}^*,0) & \partial_{x2}H_2(\mathbf{x}^*,0) & \partial_{x3}H_2(\mathbf{x}^*,0) & \partial_{x4}H_2(\mathbf{x}^*,0) & \partial_{x5}H_2(\mathbf{x}^*,0) & \partial_{x6}H_2(\mathbf{x}^*,0)\\
\partial_{x1}H_3(\mathbf{x}^*,0) & \partial_{x2}H_3(\mathbf{x}^*,0) & \partial_{x3}H_3(\mathbf{x}^*,0) & \partial_{x4}H_3(\mathbf{x}^*,0) & \partial_{x5}H_3(\mathbf{x}^*,0) & \partial_{x6}H_3(\mathbf{x}^*,0)\\
\partial_{x1}H_4(\mathbf{x}^*,0) & \partial_{x2}H_4(\mathbf{x}^*,0) & \partial_{x3}H_4(\mathbf{x}^*,0) & \partial_{x4}H_4(\mathbf{x}^*,0) & \partial_{x5}H_4(\mathbf{x}^*,0) & \partial_{x6}H_4(\mathbf{x}^*,0)\\
\partial_{x1}H_5(\mathbf{x}^*,0) & \partial_{x2}H_5(\mathbf{x}^*,0) & \partial_{x3}H_5(\mathbf{x}^*,0) & \partial_{x4}H_5(\mathbf{x}^*,0) & \partial_{x5}H_5(\mathbf{x}^*,0) & \partial_{x6}H_5(\mathbf{x}^*,0)\\
\partial_{x1}H_6(\mathbf{x}^*,0) & \partial_{x2}H_6(\mathbf{x}^*,0) & \partial_{x3}H_6(\mathbf{x}^*,0) & \partial_{x4}H_6(\mathbf{x}^*,0) & \partial_{x5}H_6(\mathbf{x}^*,0) & \partial_{x6}H_6(\mathbf{x}^*,0)
\end{pmatrix}\\
&= \mathrm{sgn}\begin{pmatrix}
0 & 0 & 0 & 0 & 0 & -\overline{\beta}e^{x_6^*}\\
\overline{\beta}e^{x_1^*+x_6^*-x_2^*} & -\overline{\beta}e^{x_1^*+x_6^*-x_2^*} & 0 & 0 & 0 & \overline{\beta}e^{x_1^*+x_6^*-x_2^*}\\
0 & \overline{\alpha}e^{x_2^*-x_3^*} & -\overline{\alpha}e^{x_2^*-x_3^*} & 0 & 0 & 0\\
0 & 0 & 0 & -\overline{\kappa}e^{x_6^*-x_4^*} & 0 & \overline{\kappa}e^{x_6^*-x_4^*}\\
0 & 0 & \overline{\nu}e^{x_3^*+x_4^*-x_5^*} & \overline{\nu}e^{x_3^*+x_4^*-x_5^*} & -\overline{\nu}e^{x_3^*+x_4^*-x_5^*} & 0\\
0 & 0 & 0 & 0 & \overline{\theta}e^{x_5^*-x_6^*} & -\overline{\theta}e^{x_5^*-x_6^*}
\end{pmatrix}
\end{aligned}
$$

$$= \operatorname{sgn}\left(2\overline{\beta}^2\overline{\alpha}\,\overline{\kappa}\,\overline{\nu}\,\overline{\theta}\,e^{x_1^*+2x_6^*}\right) = 1.$$

Then, $\deg(J\mathbb{Q}N, \Omega \cap \operatorname{Ker}(L), 0) = 1 \neq 0$. In this way, condition the item (C3) of Theorem 2.1 is verified.

3.3. Conclusion of the proof of Theorem 1.2

The existence of the solution for $L\mathbf{x} = N\mathbf{x}$ on $\operatorname{Dom}(L) \cap \overline{\Omega}$ is a straightforward consequence of the application of Theorem 2.1 since the items (C1), (C2), and (C3) are satisfied.

4. Proof of Theorem 1.1

We can rewrite the system (1.1)–(1.7) as the operator equation of the form (1.11) (see Theorem A.1) on E with the operators L and N defined in (1.9) and (1.10), respectively. Moreover, the items (C1), (C2), and (C3) of Theorem 2.1 are satisfied by Lemma 3.3. Hence, by application of Theorem 2.1 there exists at least one solution of the operator equation $L\mathbf{x} = N\mathbf{x}$ on $\operatorname{Dom}(L) \cap \overline{\Omega}$ with Ω defined on (1.13) and $\sigma = h$ (see (3.35)). Moreover, from the change of variable (1.12), we obtain the existence $\left(P_s, P_e, P_i, V_s, V_e, V_i\right)^T(t)$, which is a positive periodic solution of (1.1)–(1.7).

5. Numerical examples

In this section, the objective is to provide a general proof of concept that the governing equations can qualitatively resemble expected population dynamics, without specific adjustments for a quantitative calibration. The biological considerations related to the flavescence dorée (see, e.g., [45, 46]) serve as a general reference for the model.

The population sizes are non-dimensional, where "1" corresponds to a reference unit; the initial values are adjusted such that the corresponding species (plant or vector) sum up to "1". The time scales are adjusted to reflect the realistic scenarios of the typical life cycles based on the temporal dynamics of the following species:

- Grapevines (Vitis spp.): Grapevines are perennial plants with no specific lifespan; they can live for many years if kept healthy. Commercial vineyards typically replace grapevines after 25–30 years, as the fruit production may decline by then. Therefore, 10,000 days, which corresponds to approximately 27.4 years, can be considered a the reference timespan; for the simulations, we chose 1000 days as a the time span, which allows us to visualize three cycles.
- Flavescence dorée: This disease is caused by phytoplasma, which is a bacterium without cell walls. The phytoplasma reproduces by binary fission within the phloem of a host plant. The phloem is a tissue in vascular plants that transports soluble organic compounds from the leaves to other parts of the plant. The phytoplasma relies entirely on the grapevine for survival and reproduction and spreads to other plants only through insect vectors, such as leafhoppers.
- *Scaphoideus titanus* (leafhopper): This insect has one generation per year, with life cycle stages varying based on the hemisphere:
  - Eggs are laid in late summer (August-October in the Northern Hemisphere; February-May in the Southern Hemisphere) and over winter on the vine.

– Nymphs hatch in late spring, typically around mid-May (Northern Hemisphere) or mid-November (Southern Hemisphere) of the following year.
– Adults emerge from the final nymphal stage in mid-summer (June-July in the Northern Hemisphere; December-January in the Southern Hemisphere). During this time, they can acquire and transmit the flavescence dorée phytoplasma while feeding on the grapevine sap. Adults live for 1–3 months, dying in late summer.

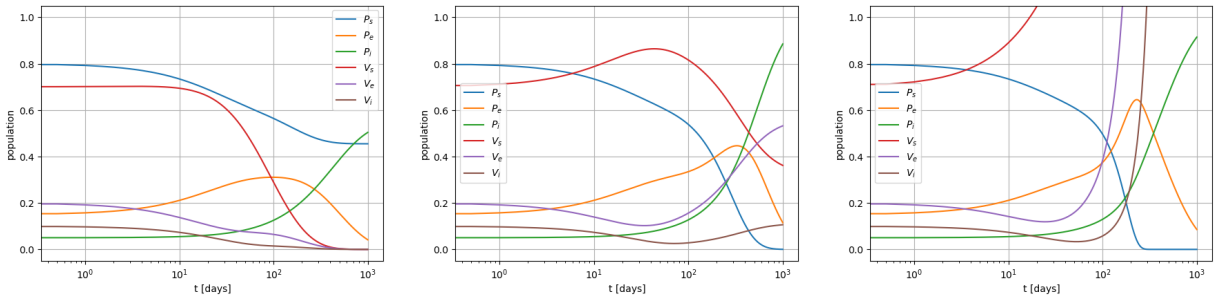

(a) (b) (c)

Figure 2. Example 1 (without periocity): Profile of simulation of plant and vector populations; (a) $\Lambda(t) \equiv 0.04$, (b) $\Lambda(t) \equiv 0.05$, (c) $\Lambda(t) \equiv 0.06$.

5.1. *Example 1*

For Example 1, the following parameter specifications are chosen:

- The life span of the vector is set to $\mu_1^{-1} = 20$ days, which corresponds to a natural mortality rate of $\mu_1 = 0.05$ (per day).
- The density-dependent mortality rate is specified as $\mu_2 = 0.001$ (per day per vector).
- For the recruitment rate, Λ, we estimate an average lifetime fecundity of approximately 30–40 eggs per female. This estimate is based on 2–4 clutches per female during their adult life, with each clutch containing 5–20 eggs. While technically not a pregnancy, but rather oviposition, the females lay eggs either singly or in small clutches within the plant tissues after mating. As a result, we estimate an egg-laying rate between 0.01 and 0.06 eggs per day, with 0.06 being an optimistic estimate and 0.01 being a more conservative rate, thereby accounting for lower egg survival rates. In the examples, the main variations operate on changes of Λ.
- The probability of transmission of the bacterium from the plant to the vector, denoted by β, is estimated at 0.1, or 10%. This value lies within a reasonable range of 2–40%.
- Similarly, the probability of transmission of the bacterium to the grapevine, denoted by ν, is also estimated at $\nu = 0.1$, which falls within the 2–40% range, thus representing the probability that the susceptible vectors become infected within a unit of time.
- The parameter θ^{-1} represents the average incubation period of the bacterium in the vector. Although the bacterium slowly multiplies within the vector after ingestion, we assume an incubation period of 30 days, which corresponds to $\theta = 1/30 \approx 0.033$. This value is adopted according to [30] (see also [47]): "An incubation period of about 1 month, during which time the

phytoplasma multiplies and colonizes the vector's body, is required before the vector becomes infectious."

- The parameter α^{-1} denotes the average incubation time of the bacterium in the grapevine. Flavescence dorée, caused by phytoplasmas, typically has an incubation period of one year or more before symptoms manifest on the grapevine. This prolonged period allows the phytoplasma to reproduce and overcome the plant defenses. We set $\alpha^{-1} = 365$, meaning $\alpha = 1/365 \approx 0.0027$.
- The recovery parameter is set to $\kappa = 0$, as no recovery occurs in the case of flavescence dorée. Once the vector (leafhopper) acquires the infection, it becomes systemic, meaning the vector remains infectious for the rest of its life, with no possibility of recovery. This corresponds to an infinite average recovery time of the vector κ^{-1}.
- The parameter γ^{-1} represents the average time the grapevine remains infectious. A grapevine infected with flavescence dorée remains infectious for its entire lifespan due to the systemic nature of the infection, which affects the entire vascular system of the vine. Hence, we set $\gamma = 0$, as the infection persists indefinitely, with no recovery or reduction in the infectivity.

The initial condition

$$x(0) = \mathbf{x}_0 = (0.8, 0.15, 0.05, 0.7, 0.2, 0.1), \tag{5.1}$$

is adjusted such that the fractions of each species (plants or vectors) adds to 1, thus providing a dominance of susceptible species. The initial values of each variable are intentionally chosen to create a visual distinction between the functions. In Examples 1(a)–(c), we select the following variations of the constant function $\Lambda(t)$: $\{0.04, 0.05, 0.06\}$. See Figure 2 for a visualization of the simulation across all variables.

The plot employs a logarithmic scale on the x-axis to capture the long-term behavior and the asymptotic trends of the plant variables P_e and P_i within the range $[100, 1000]$, while still adequately visualizing the short-term behavior of the vector variables in the range $[0, 100]$.

In Figure 2(a), for $\Lambda(t) \equiv 0.04$, all vector populations monotonically decrease and eventually vanish. This outcome is expected for smaller recruitment rates $\Lambda(t)$. The infected plant population monotonically increases towards an asymptotic value, while the susceptible plant population monotonically decreases, appearing to approach a non-zero asymptotic value. This non-zero value results from the absence of the vector populations, which would otherwise drive the susceptible plant population further down. The exposed plant population initially increases to a maximum and then declines to an asymptotic value of zero.

How do these dynamics change with an increase in the recruitment rate? This can be seen in Figure 2(b), where $\Lambda(t) \equiv 0.05$. When the recruitment rate increases, the vector populations, particularly the infected vector V_i, which does not vanish as in the previous example, but can stabilize at a non-zero level.The susceptible vectors V_s initially increase, reach a maximum, and then begin to decline. From the visualization, it is unclear whether the asymptotic value of V_s is zero; however, based on the equations, it should eventually converge to zero. The other two vector populations, V_e and V_i, first decrease, reaching a minimum (first V_e, followed by V_i), and then increase towards an asymptotic state. Additionally, the dynamics of the plant population change: in contrast to the previous example, the susceptible plant population P_s quickly vanishes within the overall time interval.

In Example 1(c), the recruitment rate is further increased to $\Lambda(t) \equiv 0.06$, thus leading to an uncontrolled rise in all vector populations, as illustrated in Figure 2(c). The qualitative behavior of the plant

population remains the same, with the notable difference being that the exposed plant population P_e exhibits a more pronounced peak.

5.2. *Example 2*

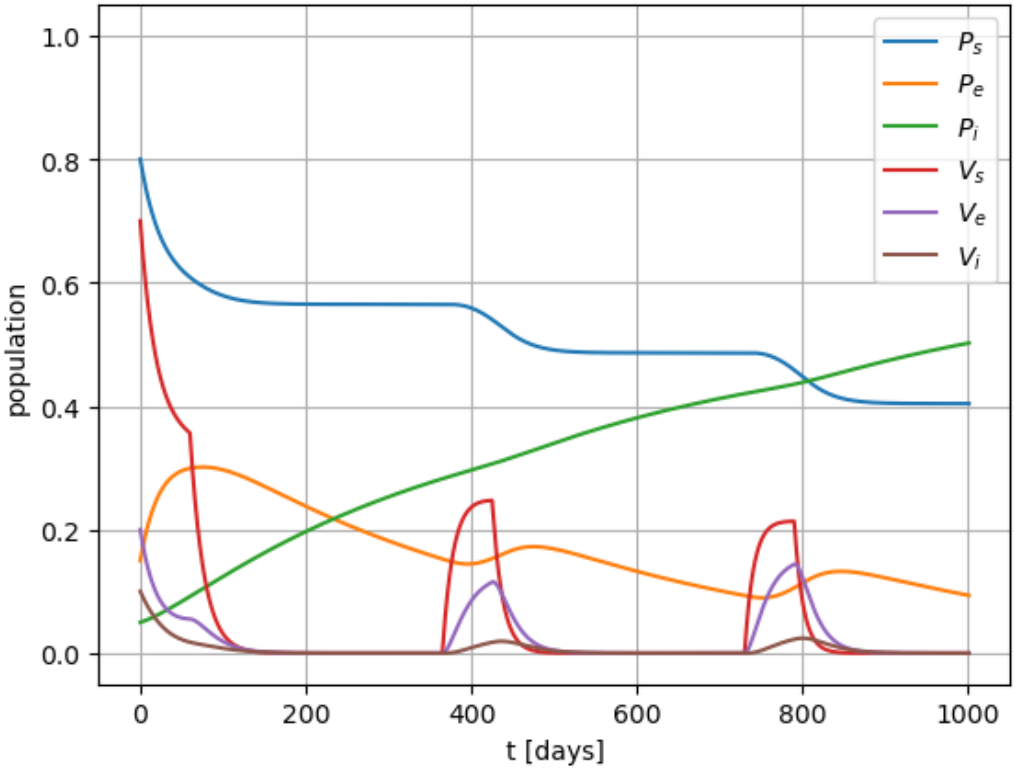

Figure 3. Example 2(a): Profile of plant and vector populations with periodic growth; $\lambda_1 = 0.02$.

In Example 2, we want to explore the effect of periodic parameters by modifying the equation that governs the susceptible vector population, V_s. The goal of this adjustment is to control the growth of the vector population. The modified equation for V_s is as follows:

$$\frac{dV_s(t)}{dt} = \Lambda(t) - (\mu_1(t) + \mu_2(t) \cdot V(t))V_s(t) - \nu(t)V_s(t),$$

where we replace the term $\Lambda(t)V$ with $\Lambda(t)$, which is now defined by the following:

$$\Lambda(t) = \lambda_1(t) + \lambda_2(t)V.$$

This modification offers a significant advantage: it makes the growth rate of V_s independent of the total vector population V. In cases where the vector population V drastically decreases, the growth of V_s is no longer tightly coupled to V, thus preventing a prolonged delay in recovery.

Then, the governing equation for $V_s(t)$ is then slightly modified:

$$\frac{dV_s(t)}{dt} = \Lambda(t) - (\mu_1(t) + \mu_2(t) * V(t))V_s(t) - \nu(t)V_s(t)P_i(t) + \kappa(t)Vi(t).$$

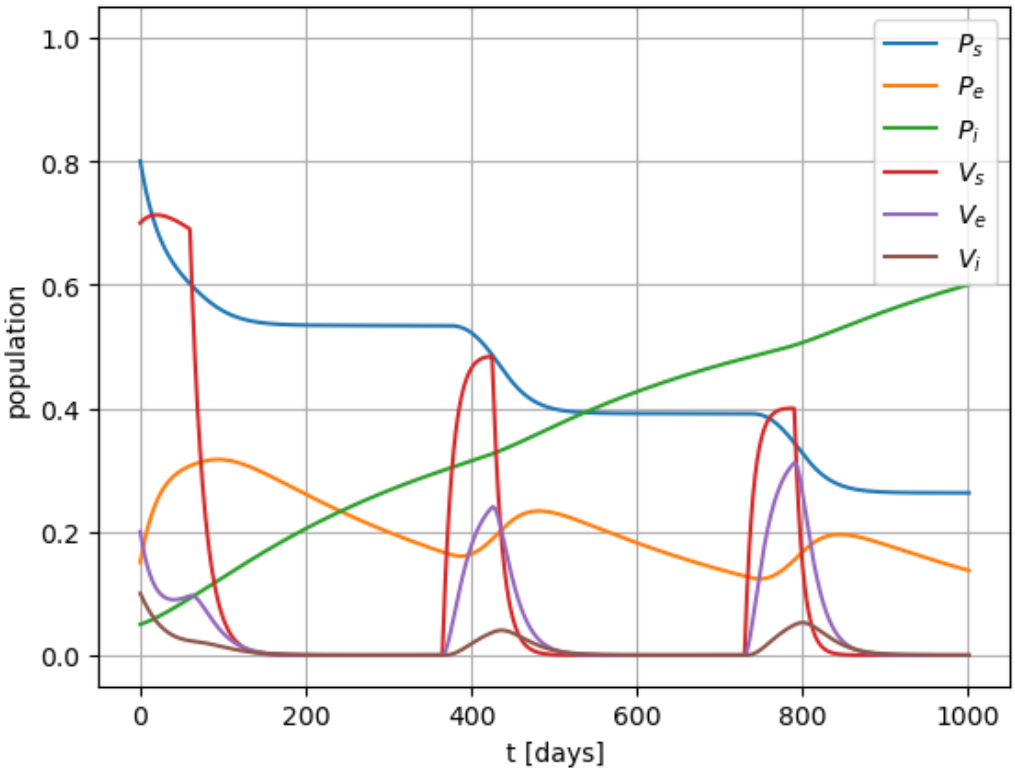

Figure 4. Example 2(b): Profile of plant and vector populations with periodic growth; $\lambda_1 = 0.02$.

In this second example, the same initial conditions are used as in Example 1, along with most of the same parameters. The primary difference is the modification of $\Lambda(t)$, which is chosen as the following periodic function:

$$\Lambda(t) = \begin{cases} \lambda_1 & \text{if} \quad (t \bmod 365) < 60, \\ 0 & \text{otherwise.} \end{cases} \tag{5.2}$$

Here, $\Lambda(t)$ is defined as active for 60 days each year (representing a seasonal factor, such as increased vector reproduction during specific months). For Example 2(a), we set $\lambda_1 = 0.02$, and we increase λ_1 to 0.04 for Example 2(b) to simulate a higher vector birth rate during the active period.

Figures 3 and 4 depict the simulations for Examples 2(a) and 2(b), respectively. These simulations illustrate the periodic behavior of the plant and vector populations over time, with varying levels of periodicity in the vector growth rate, which is controlled by the different values of λ_1.

This example demonstrates how altering the periodicity and the vector population's growth rate affects the plant-vector system's overall dynamics. By tuning parameters such as λ_1, vineyard managers or researchers could explore different scenarios, such as varying climatic conditions or vector control interventions.

The dynamics of the vector population are primarily driven by their recruitment rate, Λ, which is considered as a primary control variable, and focused on in this second example. During a typical season, the susceptible vector population V_s initially increases, thus approaching its upper carrying

capacity, which exceeds the eventual peaks of the other vector stages. As this happens, the exposed vector population V_e rises and eventually overtakes the susceptible population.

The effect of the halt in growth is immediate: a steep drop in V_s triggers a more moderate decline in V_e, thus leading to a gradual decrease in V_i. Similarly, a decrease in P_s causes a slight increase in P_e. When the growth is stopped (i.e., when $\Lambda = 0$), the susceptible population populations experience a sharp decline, immediately followed by the exposed population. This anticipates the end of the adult generation. Simultaneously, the infected population reaches its peak, and then decreases. This timing is significant: the infected population peaks just as the birth rate halts. After this point, all vector populations decline to minimal levels, thus eventually disappearing. The dynamics of the plant populations mirror those of the vector populations.

The dynamics of the plant populations mirror those of the vector populations. When the infected vectors are present – typically following a bell-shaped curve with a kink at the peak – the susceptible plant population decreases in an inverse S-shaped pattern. Conversely, when the infected vectors are absent, the number of susceptible plants remains stable.

Interestingly, the number of exposed plants decreases during periods of low vector load and slightly increases during a stronger vector presence. This decrease may seem counterintuitive: why should the plant populations change when the vectors are absent? Without a significant vector population, one would expect little change in the plant populations. However, if the exposed plants are present, then they will convert into infected plants according to the system's dynamics. In this example, we chose a relatively high initial number of exposed plants. While this higher initial value might not represent a typical real-world case, it is included here for didactic purposes to examine the behavior of the system's equations.

The increasing number of infected plants is expected, as the process is designed to be irreversible – no plant recovery is considered. A key observation is that the rate of increase in the infected plants does not noticeably change during the period of vector emergence. This didactic example is due to the relatively high number of exposed plants, which dampens any significant change in the overall percentage of infected plants.

6. Conclusions

Our model for the recruitment rate assumed that births do not occur continuously throughout the year, but are seasonally concentrated. This can be modeled using a seasonally varying function that peaks during the leafhopper's breeding season. In our model, we chose a piecewise constant function that took a positive value during the breeding season and dropped to zero outside of it. This approach is both practical and effective in the absence of detailed data. While alternative functional forms could be considered, the key factors to capture are the average length of the breeding season and the breeding intensity.

6.1. Model improvements

In this paragraph, some potential improvements to the model are discussed.

As leafhoppers progress through different life stages (eggs, nymphs, adults), these stages could be modeled with distinct variables to gain a quantitative control over their development. This distinction is reasonable since only adults can infect plants, while the other stages are crucial for tracking the ef-

fective number of future adults in the next generation. Of particular relevance are the nymph dynamics, as pathogen acquisition can occur during both the nymph and adult stages.

To better capture the leafhopper life cycle, we could introduce two key state variables: N for eggs/nymphs, which represents a latent period, and V_* for adults, which represents an active period that involves both reproduction and infection. Then, the model equations could be modified as follows:

$$\dot{N} = \lambda V - \sigma N + \dots$$
$$\dot{V}_s = \sigma N + \dots$$

In the first equation, the term λV accounts for the creation of new eggs/nymphs, and the term σN represents the transition of nymphs to adults. In the second equation, the corresponding $-\sigma N$ term accounts for the removal of nymphs as they transition to adults. The function σ could vary seasonally (e.g., with $\sigma = 0$ during the breeding season and $\sigma > 0$ during hatching).

It also might be useful to formally classify two levels of infection within the plants:

1) The overall statistics of the plant population, which indicates the percentage of plants in each infection status (i.e., whether a plant is infected or not, without specifying the severity of infection).

2) The degree of infection within an individual plant, thus acknowledging that the extent of bacterial growth within a plant influences the probability of transmission.

This distinction is valuable because the severity of infection within the individual plants can significantly affect the overall dynamics of disease spread.

6.2. Outlook on real-world applications

The findings of this study have important real-world implications for disease management and prevention in vineyards, particularly in controlling flavescence dorée. By incorporating seasonality and periodic dynamics into the mathematical model, vineyard managers can better predict the timing and intensity of disease outbreaks, thus allowing for more precise interventions. For instance, the identification of key periods when the vector population is likely to surge or when grapevines are most vulnerable to infection can inform the timing of pesticide applications, thus reducing the need for constant chemical use and lowering environmental impact. Additionally, the model's ability to simulate various control strategies—such as vector population reduction, quarantine measures, or the introduction of disease-resistant grapevines—provides vineyard managers with valuable tools to assess the effectiveness of these approaches before implementation. This leads to more sustainable and cost-effective practices, as well as better long-term vineyard health, thereby reducing crop losses and increasing productivity. Ultimately, the integration of such modeling into disease management programs enhances the decision-making processes, thus aligning with the broader goals of sustainable agriculture.

Author contributions

A. Coronel, F. Huancas: Supervision; A. Coronel, F. Huancas, R. Vidal: Methodology, Writing-original draft, Visualization; A. Coronel, F. Huancas, R. Vidal, S. Berres, H. Brito: Conceptualization, Formal analysis, Investigation, Writing-review & editing; A. Coronel, F. Huancas, S. Berres: Funding acquisition. All authors have read and agreed to the published version of the manuscript.

Use of AI tools declaration

The authors declare they have not used Artificial Intelligence (AI) tools in the creation of this article. However, the authors declare to have used as Artificial Intelligence (AI) tools, namely ChatGPT for cross-checking and specifically for improving the grammar throughout the paper.

Acknowledgments

This work is partially supported by the Agencia Nacional de Investigación y Desarrollo, ANID-Chile, through the project FONDECYT 1230560 and by the Universidad Tecnológica Metropolitana through the program Proyectos Regulares de Investigación, año 2023, código LPR23-03.

Conflict of interest

The authors declare that they have no conflict of interest.

References

1. H. González, Specialization on a global scale and agrifood vulnerability: 30 years of export agriculture in Mexico, *Dev. Stud. Res.*, **1** (2014), 295–310. https://doi.org/10.1080/21665095.2014.929973
2. A. M. Buainain, M. R. Sousa, Z. Navarro, *Globalization and Agriculture: Redefining Unequal Development*, Lexington Books, USA, 2017.
3. D. R. Krichker, O. A. Ruschitskaya, The formation and development of priority exports of organic products of agro-industrial complex of the urals region, *AIP Conf. Proc.*, **2921** (2023), 090006. https://doi.org/10.1063/5.0164569
4. K. Anderson, *The World's Wine Markets: Globalization at Work,* Edward Elgar Publishing, UK, 2004. https://doi.org/10.4337/9781845420765.00001
5. G. Campbell, N. Guibert, *Wine, Society, and Globalization: Multidisciplinary Perspectives on the Wine Industry*, Palgrave Macmillan, NY, 2007. https://doi.org/10.1057/9780230609907
6. M. Berns, A.Townend, Z. Khayat, B. Balagopal, M. Reeves, M. S. Hopkins, et al., Sustainability and competitive advantage, *Sloan Manage. Rev.*, **51** (2009), 19–26.
7. J. Carrillo-Hemosilla, P. del Rio, T. Könnölä, Diversity of eco-innovations: reflections from selected case studies, *J. Cleaner Prod.*, **18** (2010), 1073–1083. https://doi.org/10.1016/j.jclepro.2010.02.014
8. A. Gilinsky, S. K. Newtona, R. F. Vega, Sustainability in the global wine industry: concepts and cases, *Agric. Agric. Sci. Procedia*, **8** (2016), 37–49. https://doi.org/10.1016/j.aaspro.2016.02.006
9. E. Fleming, S. Mounter, B. Grant, G. Griffith, R. Villano, The new world challenge: Performance trends in wine production in major wine-exporting countries in the 2000s and their implications for the Australian wine industry, *Wine Econ. Policy*, **3** (2014), 115–126. https://doi.org/10.1016/j.wep.2014.12.002

10. J. M. Núñez, A. Espejo, F. J. Fuentes, New scenario for the Spanish wine sector, International strategic perspectives, (in Spanish) *Boletín económico de ICE*, **3068** (2015), 57–67. https://doi.org/10.32796/bice.2015.3068.5512

11. F. Lessio, A. Portaluri, F. Paparella, A. Alma, A mathematical model of flavescence dorée epidemiology, *Ecol. Modell.*, **312** (2015), 41–53. https://doi.org/10.1016/j.ecolmodel.2015.05.014

12. F. Lessio, A. Alma, Models applied to grapevine pests: A review, *Insects*, **12** (2021), 169. https://doi.org/10.3390/insects12020169

13. A. Alma, F. Lessio, H. Nickel, Insects as phytoplasma vectors: Ecological and epidemiological aspects, in *Phytoplasmas: Plant Pathogenic Bacteria - II*, Springer, Singapore, (2019), 1–25. https://doi.org/10.1007/978-981-13-2832-9_1

14. G. Daglio, Potential field detection of flavescence dorée and esca diseases using a ground sensing optical system, *Biosyst. Eng.*, **215** (2022), 203–214. https://doi.org/10.1016/j.biosystemseng.2022.01.009

15. F. Tacoli, N. Mori, A. Pozzebon, E. Cargnus, S. Da Viá, P. Zandigiacomo, et al., Control of scaphoideus titanus with natural products in organic vineyards, *Insects*, **8** (2017), 129. https://doi.org/10.3390/insects8040129

16. J. Kranz, *Epidemics of Plant Diseases Mathematical Analysis and Modeling,* Springer Berlin, Heidelberg, 2004. https://doi.org/10.1007/978-3-642-75398-5

17. F. Brauer, C. Castillo-Chavez, Z. Feng, *Mathematical Models in Epidemiology*, Springer New York, NY, 2019. https://doi.org/10.1007/978-1-4939-9828-9

18. H. Fang, M. Wang, T. Zhou, Existence of positive periodic solution of a hepatitis B virus infection model, *Math. Methods Appl. Sci.*, **38** (2015), 188–196. https://doi.org/10.1002/mma.3074

19. J. Lourenço, M. Maia de Lima, N. R. Faria, A. Walker, U. MOritz, C. J. Villabona-Arenas, et al., Epidemiological and ecological determinants of Zika virus transmission in an urban setting, *eLife*, **6** (2017), e29820. https://doi.org/10.7554/eLife.29820

20. R. Ranjan, Predictions for COVID-19 outbreak in India using epidemiological models, *MedRxiv*, **2020** (2020), 11. https://doi.org/10.1101/2020.04.02.20051466

21. M. Martcheva, *An Introduction to Mathematical Epidemiology*, Springer New York, NY, 2015. https://doi.org/10.1007/978-1-4899-7612-3

22. T. Smith, G. F. Killeen, N. Maire, A. Ross, L. Molineaux, F. Tediosi, et al., Mathematical modeling of the impact of malaria vaccines on the clinical epidemiology and natural history of Plasmodium falciparum malaria: Overview, *Am. J. Trop. Med. Hyg.*, **75** (2010), 1–10. https://doi.org/10.4269/ajtmh.2006.75.2_suppl.0750001

23. W. O. Kermack, A. G. McKendrick, A contribution to the mathematical theory of epidemics, *Proc. R. Soc. London Ser. A Math. Phys. Eng. Sci.*, **115** (1927), 700–721. https://doi.org/10.1098/rspa.1927.0118

24. R. M. Anderson, R. M. May, *Infectious Diseases of Humans: Dynamics and Control*, Oxford University Press, UK, 1992. https://doi.org/10.1093/oso/9780198545996.001.0001

25. H. W. Hethcote, The mathematics of infectious diseases, *SIAM Rev.*, **42** (2000), 599–653. https://doi.org/10.1137/S0036144500371907

26. M. J. Keeling, P. Rohani, *Modeling Infectious Diseases in Humans and Animals*, Princeton University Press, UK, 2011. https://doi.org/10.2307/j.ctvcm4gk0
27. D. H. Anderson, Compartmental modeling and tracer kinetics, in *Lecture Notes in Biomathematics*, Springer-Verlag Berlin, Heidelberg, 1983. https://doi.org/10.1007/978-3-642-51861-4
28. R. Anguelov, J. Lubuma, Y. Dumont, Mathematical analysis of vector-borne diseases on plants, in *IEEE, 4th International Symposium on Plant Growth Modeling, Simulation, Visualization and Applications*, Shanghai, China, (2012), 22–29. https://doi.org/10.1109/PMA.2012.6524808
29. I. M. Bulai, A. C. Esteves, F. Lima, E. Venturino, A mathematical modeling approach to assess biological control of an orange tree disease, *Appl. Math. Lett.* **118** (2021), 107–140. https://doi.org/10.1016/j.aml.2021.107140
30. J. Chuche, D. Thiéry, Biology and ecology of the flavescence dorée vector Scaphoideus titanus: a review, *Agron. Sustainable Dev.*, **34** (2014), 381–403. https://doi.org/10.1007/s13593-014-0208-7
31. I. M. Lee, R. Gundersen, E. Dawn, R. Davis, I. Bartoszyk, Revised classification scheme of phytoplasmas based on RFLP analyses of 16S rRNA and ribosomal protein gene sequences, *Int. J. Syst. Evol. Microbiol.*, **48** (1998), 1153–1169. https://doi.org/10.1099/00207713-48-4-1153
32. A. B. Santander, E. M. Rodríguez, C. D. Toapanta, R. A. Suárez, Vitis vinifera, a case of study at Chaupi Estancia, Pichincha province, *Siembra*, **9** (2022), e3731. https://doi.org/10.29166/siembra.v9i2.3731
33. W. Sinclair, H. Griffiths, I. M. Lee, Mycoplasmalike organisms as causes of slow growth and decline of trees and shrubs, *J. Arboric.*, **20** (1994), 176–189. https://doi.org/10.48044/jauf.1994.033
34. M. Maixner, R. C. Pearson, E. Boudon-Padieu, A. Caudwelland, Scaphoideus titanus, a possible vector of grapevine yellows in New York, *Plant Dis.*, **77** (1993), 408–413. https://doi.org/10.1094/PD-77-0408
35. M. Ripamonti, M. Pegoraro, M. Rossi, N. Bodino, D. Beal, L. Panero, et al., Prevalence of flavescence dorée phytoplasma-infected scaphoideus titanus in different vineyard agroecosystems of Northwestern Italy, *Insects*, **11** (2020), 301. https://doi.org/10.3390/insects11050301
36. I. E. Rigamonti, M. Salvetti, P. Girgenti, P. A. Bianco, F. Quaglino, Investigation on flavescence dorée in north-western Italy identifies Map-M54 (16SrV-D/Map-FD2) as the only phytoplasma genotype in Vitis vinifera L. and reveals the presence of new putative reservoir plants, *Biology*, **12** (2023), 1216. https://doi.org/10.3390/biology12091216
37. S. Tramontini, A. Delbianco, S. Vos, Pest survey card on flavescence dorée phytoplasma and its vector scaphoideus titanus, *EFSA Supporting Publ.*, **17** (2020), 1909E. https://doi.org/10.2903/sp.efsa.2020.EN-1909
38. M. Ripamonti, M. Pegoraro, C. Morabito, I. Gribaudo, A. Schubert, D. Bosco, et al., Susceptibility to flavescence dorée of different Vitis vinifera genotypes from north-western Italy, *Plant Pathol.*, **77** (2021), 511–520. https://doi.org/10.1111/ppa.13301
39. R. Gaines, J. Mawhin, *Coincidence Degree and Nonlinear Differential Equations*, Springer–Verlag, Berlin, Germany, 1977. https://doi.org/10.1007/BFb0089537
40. P. Benevieri, M. Furi, A simple notion of orientability for Fredholm maps of index zero between Banach manifolds and degree theory, *Ann. Sci. Math. Québec*, **22** (1998), 131–148.

41. G. Dinca, J. Mawhin, Brouwer degree: The core of nonlinear analysis, in *Progress in Nonlinear Differential Equations and Their Applications*, Birkhäuser Cham, Switzerland, **95** (2021). https://doi.org/10.1007/978-3-030-63230-4

42. A. Coronel, F. Huancas, M. Pinto, Sufficient conditions for the existence of positive periodic solutions of a generalized nonresident computer virus model, *Quaestiones Math.*, **44** (2019), 259–279. https://doi.org/10.2989/16073606.2019.1686438

43. A. Coronel, F. Huancas, I. Hess, E. Lozada, F. Novoa-Muñoz, Analysis of a SEIR-KS mathematical model for computer virus propagation in a periodic environment, *Mathematics*, **8** (2020), 761. https://doi.org/10.3390/math8050761

44. A. Coronel, F. Huancas, S. Berres, Study of an epidemiological model for plant virus diseases with periodic coefficients, *Appl. Sci.*, **14** (2024), 399. https://doi.org/10.3390/app14010399

45. J. Chuche, D. Thiery, Biology and ecology of the Flavescence dorée vector Scaphoideus titanus: A review, *Agron. Sustainable Dev.*, **34** (2014), 355–377. https://doi.org/10.1007/s13593-014-0208-7

46. S. Tramontini, A. Delbianco, S. Vos, Pest survey card on flavescence dorée phytoplasma and its vector Scaphoideus titanus, *EFSA Supporting Publ.*, **17** (2020), 36. https://doi.org/10.2903/sp.efsa.2020.EN-1909

47. E. Boudon-Padieu, Cicadelle vectrice de la flavescence dorée, *Scaphoideus Titanus*, Ball, 1932, in *Ravageurs de la vigne*, Féret, Bordeaux, (2000), 110–120.

48. S. Malembic-Maher, P. Salar, L. Filippin, P. Carle, E. Angelini, X. Foissac, Genetic diversity of European phytoplasmas of the 16SrV taxonomic group and proposal of 'Candidatus Phytoplasma rubi', *Int. J. Syst. Evol. Microbiol.*, **61** (2011), 2129–2134. https://doi.org/10.1099/ijs.0.025411-0

Appendix

A. Reformulation of the system (1.1)–(1.7) as operator equation

Theorem A.1. *Consider that the hypothesis of Theorem 1.1 are satisfied. Let L and N be the operators defined in* (1.9) *and* (1.10)*, Respectively, and consider* $\mathbf{x}(t) = (x_1, \ldots, x_6)^T(t)$ *defined by* (1.12)*. Then, the following statements are true:*

(a) $\mathbf{x}$ *is a solution of the operator equation* (1.11) *if and only if a solution of* $(P_s, P_e, P_I, V_s, V_e, V_i)$ *is a solution of the system* (1.1)–(1.7).

(b) If the solution of (1.11) *is* $\omega-$*periodic, then the solution of system* (1.1)–(1.7) *is also* $\omega-$*periodic.*

(c) If operator equation (1.11) *has a solution. Then system* (1.1)–(1.7) *has a positive solution.*

Proof. In order to prove Theorem A.1-(a), we begin by noticing that the change of variable (1.12) and differentiation imply the following identities:

$$\frac{d}{dt}\mathbf{x}(t) = \frac{1}{P}\Big(e^{-x_1(t)}\frac{dP_s}{dt}, e^{-x_2(t)}\frac{dP_e}{dt}, e^{-x_3(t)}\frac{dP_i}{dt}, e^{-x_4(t)}\frac{dV_s}{dt}, e^{-x_5(t)}\frac{dV_e}{dt}, e^{-x_6(t)}\frac{dV_i}{dt}\Big)(t), \tag{A.1}$$

$$\frac{d}{dt}\Big(P_s, P_e, P_i, V_s, V_e, V_i\Big) = \Big(Pe^{x_1}\frac{dx_1}{dt}, Pe^{x_2}\frac{dx_2}{dt}, Pe^{x_3}\frac{dx_3}{dt}, Pe^{x_4}\frac{dx_4}{dt}, Pe^{x_5}\frac{dx_5}{dt}, Pe^{x_6}\frac{dx_6}{dt}\Big). \tag{A.2}$$

If $(P_s, P_e, P_i, V_s, V_e, V_i)^T$ is a solution of system (1.1)–(1.7), then using (A.1) and (1.12), we deduce that $\mathbf{x}$ is a solution of the following system:

$$\frac{dx_1}{dt} = -\beta(t)e^{x_6} + \gamma e^{x_3-x_1}, \tag{A.3}$$

$$\frac{dx_2}{dt} = \beta(t)e^{x_6+x_1+x_2} - \alpha, \tag{A.4}$$

$$\frac{dx_3}{dt} = \alpha e^{x_2-x_3} - \gamma, \tag{A.5}$$

$$\frac{dx_4}{dt} = \Lambda(t)\Big(e^{x_4} + e^{x_5} + e^{x_6}\Big)e^{-x_4} - \Big(\mu_1 + \mu_2 P\Big(e^{x_4} + e^{x_5} + e^{x_6}\Big)\Big) - \nu(t)e^{x_3} + \kappa e^{x_6-x_4}, \tag{A.6}$$

$$\frac{dx_5}{dt} = -\Big(\mu_1 + \mu_2 P\Big(e^{x_4} + e^{x_5} + e^{x_6}\Big)\Big) + \nu(t)e^{x_4+x_3-x_5} - \theta, \tag{A.7}$$

$$\frac{dx_6}{dt} = -\Big(\mu_1 + \mu_2 P\Big(e^{x_4} + e^{x_5} + e^{x_6}\Big)\Big) + \theta e^{x_5-x_6} - \kappa, \tag{A.8}$$

$$\mathbf{x}(0) = \left(\ln\Big(\frac{P_s^0}{P}\Big),\ \ln\Big(\frac{P_e^0}{P}\Big),\ \ln\Big(\frac{P_i^0}{P}\Big),\ \ln\Big(\frac{V_s^0}{P}\Big),\ \ln\Big(\frac{V_e^0}{P}\Big),\ \ln\Big(\frac{V_i^0}{P}\Big)\right). \tag{A.9}$$

Using the operators L and N defined in (1.9) and (1.10), respectively, we can rewrite the system (A.3)–(A.9) as the operator equation (1.11). Conversely, if we consider that $\mathbf{x}$ satisfies (1.11), we deduce that $\mathbf{x}$ is a solution of (A.3)–(A.9); then by the application of (A.2) and (1.12),we get that $(P_s, P_e, P_i, V_s, V_e, V_i)^T$ is a solution of system (1.1)–(1.7).

The proofs of items (b) and (c) of Theorem A.1 are straightforward consequence of (1.12).

B. Proof of Lemma 2.1

(a) Let $\mathbf{x} \in \operatorname{Ker}(L)$, (i.e., $L(\mathbf{x}) = \mathbf{0} \in \mathbb{R}^6$). Then, by the definition of the operator L, we deduce that $\mathbf{x}'(t) = \mathbf{0}$, or equivalently that $\mathbf{x}(t) = \mathbf{x}(0)$ for $t \in [0, \omega]$. Thus, we deduce that $\operatorname{Ker}(L) \cong \mathbb{R}^6$ and $dim(\operatorname{Ker}(L)) = 6 < \infty$. Applying the elementary algebra results, we obtain the following: (i) $X \cong \operatorname{Ker}(L) \bigoplus (X/\operatorname{Ker}(L))$; (ii) $Y \cong \operatorname{Im}(L) \bigoplus (X/\operatorname{Ker}(L)) \cong \operatorname{Im}(L) \bigoplus (Y/\operatorname{Ker}(L))$, since $X = Y$; and (iii) $\operatorname{Im}(L) \cong (X/\operatorname{Ker}(L))$. Using (iii) in (i), it follows that $X \cong \operatorname{Ker}(L) \bigoplus (X/\operatorname{Ker}(L)) \cong \operatorname{Ker}(L) \bigoplus \operatorname{Im}(L)$; and from (ii), $Y \cong (Y/\operatorname{Ker}(L)) \bigoplus \operatorname{Im}(L)$, which implies that $\operatorname{Ker}(L) \cong (Y/\operatorname{Ker}(L))$ using the fact that $X = Y$. Therefore, $dim(\operatorname{Ker}(L)) = dim(Y/\operatorname{Ker}(L)) = codim(\operatorname{Im}(L)) = 6 < \infty$.

In order to prove that $\operatorname{Im}(L)$ is a closed set, we select arbitrarily $\mathbf{y} \in \operatorname{Im}(L)$. Then, we can find $\mathbf{x} \in \operatorname{Dom}(L)$ such that $L(\mathbf{x}) = \mathbf{y}$, and by the definition of L and the fact that $\mathbf{x} \in X$, we deduce the following

$$L(\mathbf{x}) = \mathbf{y} \quad \Leftrightarrow \quad \frac{d\mathbf{x}(t)}{dt} = \mathbf{y}(t) \quad \Leftrightarrow \quad \int_t^{t+\omega} d\mathbf{x} = \int_t^{t+\omega} \mathbf{y}(\tau)d\tau \quad \Leftrightarrow \quad \mathbf{0} = \int_t^{t+\omega} \mathbf{y}(\tau)d\tau.$$

Equivalently, $\operatorname{Im}(L)$ is characterized by $\operatorname{Im}(L) = \Big\{\mathbf{y} \in Y : \int_0^{\omega} \mathbf{y}(\tau)d\tau = \mathbf{0}\Big\}$. Moreover, it follows that for a continuous $f : \operatorname{Im}(L) \subset X \to \mathbb{R}^6$; $f^{-1}(\mathbf{0}^T) = \operatorname{Im}(L)$ is a closed set; because $\Big\{\mathbf{0}^T\Big\}$ is a closed set of $\mathbb{R}^6$.

Hence, we have that L is a Fredholm operator of index zero.

(b) Consider the sequence $\{\mathbf{x}_n\} \subset X$ and $\overline{\mathbf{x}} \in X$ such that $\mathbf{x}_n \to \overline{\mathbf{x}}$ in the topology induced by the norm of X. Based on the definition of the operator N as given in (1.10), and applying the inequality component-wise,

$$|\exp(z_2) - \exp(z_1)| = \left| \int_{z_2}^{z_1} \exp(s)ds \right| \leq \max\left\{ \exp(z_1), \exp(z_2) \right\} |z_2 - z_1|, \quad \forall z_1, z_2 \in \mathbb{R},$$

we establish the existence of a constant $C > 0$ depending only on ψ, ϕ, ν, θ, α, β, γ, and κ, such that $\|N(\mathbf{x}_n) - N(\overline{\mathbf{x}})\| \leq C\|\mathbf{x}_n - \overline{\mathbf{x}}\|$. This leads to the conclusion that $N(\mathbf{x}_n) \to N(\overline{\mathbf{x}})$ in the norm of E, proving that N is continuous.

(c) By the definition of the operator $\mathbb{P}$, we easily deduce that it is linear, continuous, and is a projector, since

$$\begin{aligned}\mathbb{P}^2(\mathbf{x}) = \mathbb{P}(\mathbb{P}(\mathbf{x})) = \mathbb{P}\left(\frac{1}{\omega}\int_0^\omega \mathbf{x}(\tau)d\tau\right) = \frac{1}{\omega}\int_0^\omega \frac{1}{\omega}\int_0^\omega \mathbf{x}(\tau)d\tau ds = \frac{1}{\omega}\int_0^\omega ds \cdot \frac{1}{\omega}\int_0^\omega \mathbf{x}(\tau)d\tau \\ = \frac{\omega}{\omega}\frac{1}{\omega}\int_0^\omega \mathbf{x}(\tau)d\tau = \frac{1}{\omega}\int_0^\omega \mathbf{x}(\tau)d\tau = \mathbb{P}(\mathbf{x}).\end{aligned}$$

Using the fact that $\mathbb{P} = \mathbb{Q}$, we have the same conclusions for the operator $\mathbb{Q}$ (i.e., $\mathbb{Q}$ is linear, continuos and is a projector).

We prove that $\mathrm{Ker}\,(L) = \mathrm{Im}\,(\mathbb{P})$ by using the double inclusion argument. We can deduce that $\mathrm{Ker}\,(L) \subset \mathrm{Im}\,(\mathbb{P})$; by the results of Lemma 2.1–*(a)*, we can apply the following arguments: if $\mathbf{x} \in \mathrm{Ker}\,(L) \cong \mathbb{R}^6$, then we have that $\mathbf{x}(t)$ is a constant function on $[0, \omega]$, then $\mathbb{P}(\mathbf{x}) = \mathbf{x}$ or equivalently $\mathbf{x} \in \mathrm{Im}\,(\mathbb{P})$. Conversely, we prove that $\mathrm{Im}\,(\mathbb{P}) \subset \mathrm{Ker}\,(L)$ as follows: if $\mathbf{y} \in \mathrm{Ker}\,(L)$, then there exists $\mathbf{z} \in X$ such that $\mathbb{P}(\mathbf{z}) = \mathbf{y}$; and from the definition of $\mathbb{P}$, we get $\omega^{-1}\int_0^\omega \mathbf{z}(\tau)d\tau = \mathbf{y}$, i.e., $L(\mathbf{y}) = \mathbf{0}$, which implies that $\mathbf{y} \in \mathrm{Ker}\,(L)$.

We prove that $\mathrm{Ker}\,(\mathbb{Q}) = \mathrm{Im}\,(L)$ using the definition of the operator $\mathbb{Q}$ and the characterization of $\mathrm{Im}\,(L)$ given on the item (a): $\mathbf{y} \in \mathrm{Ker}\,(\mathbb{Q})$ is equivalent to $\int_0^\omega \mathbf{y}(\tau)d\tau = \mathbf{0}$ or $\mathbf{y} \in \mathrm{Im}\,(L)$.

To prove $\mathrm{Im}\,(I - \mathbb{Q}) = \mathrm{Im}\,(L)$, we consider $\mathbf{y} \in \mathrm{Im}\,(I - \mathbb{Q})$; then, there exists $\mathbf{z} \in X$ such that

$$(I - \mathbb{Q})\Big(\mathbf{z}\Big) = \mathbf{y} \;\Leftrightarrow\; \int_0^\omega \left(\mathbf{z}(\tau) - \frac{1}{\omega}\int_0^\omega \mathbf{z}(m)dm\right)d\tau = \int_0^\omega \mathbf{y}(\tau)d\tau = \mathbf{0} \;\Leftrightarrow\; \mathbf{y}(\tau) \in \mathrm{Im}\,(L).$$

The last equivalence is obtained by the application of item (a). Hence, we deduce that $\mathrm{Im}\,(I - Q) = \mathrm{Im}\,(L)$.

Let us prove the existence of the Operators K_P and L_P. The operator L_P is the restriction of L to $\mathrm{Dom}\,(L) \cap \mathrm{Ker}\,(\mathbb{P})$ (i.e., $L_P : \mathrm{Dom}\,(L) \cap \mathrm{Ker}\,(\mathbb{P}) \to \mathrm{Im}\,(L)$ and $L_P = L$ on $\mathrm{Dom}\,(L) \cap \mathrm{Ker}\,(\mathbb{P})$). The operator K_P is the inverse operator of L_P, defined by the following relation:

$$K_P(\mathbf{x})(t) = \int_0^t \mathbf{x}(\tau)d\tau - \frac{1}{\omega}\int_0^\omega \int_0^\eta \mathbf{x}(m)dmd\eta. \tag{B.1}$$

To prove that $K_P = L_P^{-1}$, we apply the following identity:

$$\int_0 \frac{d}{ds}\mathbf{x}(s)ds - \frac{1}{\omega}\int_0^\omega \int_0 \frac{d}{dm}\mathbf{x}(m)dmdt = \mathbf{x}(t),$$

which is satisfied only on $\text{Dom}\,(L) \cap \text{Ker}\,(\mathbb{P})$.

(d) Considering the definition of the operator $\mathbb{Q}$, we note that $\mathbb{Q}N(\mathbf{x}) = \frac{1}{\omega}\int_0^\omega N(\tau)d\tau$. Then, for $\mathbf{x} \in \overline{\Omega}$ we get that $\|\mathbb{Q}N(\mathbf{x})\| \leq \frac{1}{\omega}\int_0^\omega \|N\|d\tau = \|N\|$, which implies that $\mathbb{Q}N(\overline{\Omega})$ is bounded on $\overline{\Omega}$. From the definitions of the operators K_P, N and $\mathbb{Q}$, we have the following:

$$\Big(K_P(I-\mathbb{Q})N)\Big)(\mathbf{x})(t) = \int_0^t N(\tau)d\tau + \left(\frac{1}{2} - \frac{t}{\omega}\right)\int_0^\omega N(\tau)d\tau - \frac{1}{\omega}\int_0^\omega \int_0^\eta N(m)dmd\eta.$$

Consequently, we deduce the estimate $\|K_P(I-\mathbb{Q})N\| \leq 3\omega\|N\|$, thus indicating that $(K_P(I-\mathbb{Q})N)(\overline{\Omega})$ is bounded on $\overline{\Omega}$, as N is bounded on $\overline{\Omega}$. Additionally, we clearly deduce that

$$\Big|\Big(K_P(I-\mathbb{Q})N)\Big)(\mathbf{x})(t) - \Big(K_P(I-\mathbb{Q})N)\Big)(\mathbf{x})(s)\Big| \leq 2\|N\|\,|t-s|, \quad \forall t, s \in [t_0, \infty],$$

or equivalently, $K_P(I-\mathbb{Q})N$ is an equicontinuous operator. By applying Arzela-Ascoli's theorem, it follows that $K_P(I-\mathbb{Q})N$ is a compact operator on $\overline{\Omega}$. Thereby, we conclude that N is L-compact on $\overline{\Omega}$.